DAHLGREN DIVISION
NAVAL SURFACE WARFARE CENTER
Dahlgren, Virginia 22448-5100

NSWCDD/TR-95/196

PRECISE ABSOLUTE NAVIGATION: AN EVALUATION OF PPS POSITION MANAGEMENT

BY BRUCE R. HERMANN BONNIE S. RISINGER

STRATEGIC AND SPACE SYSTEMS DEPARTMENT

OCTOBER 1995

REPORT DOCUMENTATION PAGE

Form Approved
OMB No. 0704-0188

1. AGENCY USE ONLY (Leave blank)	2. REPORT DATE	3. REPORT TYPE AND DATES COVERED
	October 1995	Draft

4. TITLE AND SUBTITLE

Precise Absolute Navigation: An Evaluation of PPS Position Improvement

5. FUNDING NUMBERS

6. AUTHOR(s)

B. Hermann, B. Risinger

7. PERFORMING ORGANIZATION NAME(S) AND ADDRESS(ES)

Commander
Naval Surface Warfare Center
Dahlgren Division (Code K12)
17320 Dahlgren Road
Dahlgren, VA 22448-5100

8. PERFORMING ORGANIZATION REPORT NUMBER

NSWCDD/TR-95/196

9. SPONSORING/MONITORING AGENCY NAME(S) AND ADDRESS(ES)

Defense Mapping Agency Applications and Technology Group
Attn: Mr. S. Malys
ATIR MS D-84
4600 Sangamore Road
Bethesda, MD 20816-5003

10. SPONSORING/MONITORING AGENCY REPORT NUMBER

11. SUPPLEMENTARY NOTES

12a. DISTRIBUTION/AVAILABILITY STATEMENT

Approved for public release, distribution is unlimited.

12b. DISTRIBUTION CODE

13. ABSTRACT (Maximum 200 words)

This report demonstrates a method whereby the Precise Positioning Service (PPS) solutions recorded in the field can be reprocessed at a later time with precise ephemerides. The reprocessing with precise ephemerides improves the quality of the navigation solutions compared with the solutions obtained when the broadcast ephemerides are used.

The Precise Absolute Navigation (PAN) algorithm described in this paper avoids the need to reprocess the Selective Availability-(SA-) corrected observations. However, the following are required: access to the SA-corrected broadcast ephemerides for the time of interest, the postfit precise ephemerides, the PPS navigation solutions to be corrected, the Global Positioning System (GPS) time of each solution, and a list of the satellites used.

The PAN algorithm is described and its effectiveness tested with PPS-equivalent navigation solutions. The precise satellite ephemerides chosen for the navigation improvements are the DMA precise ephemerides and clock solutions. The true absolute position at each observation is either a given static point or was obtained from the on-the-fly (OTF) kinematic relative position solutions referenced to a known absolute point.

14. SUBJECT TERMS

precise ephemerides, broadcast ephemerides, PPS track, satellite, pseudo-code, GPS, Global Positioning System, pseudorange, SPS

15. NUMBER OF PAGES

70

16. PRICE CODE

17. SECURITY CLASSIFICATION OF REPORTS	18. SECURITY CLASSIFICATION OF THIS PAGE	19. SECURITYCLASSIFICATION OF ABSTRACT	20. LIMITATION OF ABSTRACT
UNCLASSIFIED	UNCLASSIFIED	UNCLASSIFED	UL

FOREWORD

A mission of the Defense Mapping Agency (DMA) requires determining geodetic-quality absolute positions autonomously and in areas far removed from other sites. The use of Differential Global Positioning Systems (DGPS) techniques or relative positioning is sometimes precluded. Operating in an unclassified mode, keyed receivers can output Precise Positioning Service (PPS) navigation solutions. Because they are computed in real time, PPS solutions necessarily use the broadcast ephemerides and consequently are subject to ephemerides and satellite-clock prediction errors. The PPS solutions can be recorded, but the broadcast ephemerides and the observations, when corrected for Selective Availability (SA), cannot. This report demonstrates a method whereby the field-recorded PPS solutions can be reprocessed with the more accurate precise ephemerides. Reprocessing with the precise ephemerides offers improved quality in navigation solutions, but does not require that the SA-corrected pseudorange or phase observations be saved. This method is called Precise Absolute Navigation (PAN).

Support for this project was provided by the DMA under the direction of Mr. B. Roth and Mr. S. Malys.

The authors wish to thank Dr. Randall Smith of DMA for suggesting this unique investigation. The authors also wish to thank the following individuals: Mr. Brian Tallman, Mr. Kim Kangas, and Mr. Brian Hagan of the DMA Aerospace Center for providing the seven days of static test data; Ms. Lisa McCormick, Ms. Mary Carroll, and Mr. David Hanson of the DMA Aerospace Center for correcting the Drive-By data in the Data Correction Facility (DCF); and Dr. Alan G. Evans of the Naval Surface Warfare Center, Dahlgren Division for providing the Drive-By data used for the dynamic testing.

This final report for FY95 has been reviewed by Dr. J. Blanton, Head, Space and Geodesy Branch and Mr. J. Sloop, Head, Space and Surface Systems Division.

Approved by:

D. B. COLBY, Head
Strategic and Space Systems Department

CONTENTS

ILLUSTRATIONS

ILLUSTRATIONS (Continued)

TABLES

MOTIVATION

The purpose of the Precise Absolute Navigation (PAN) development was to investigate the feasibility of improving, by postprocessing, the accuracy of a set of typical Precise Positioning Service (PPS) navigation solutions. Real-time, stand-alone navigation solutions necessarily use the broadcast ephemerides as the source of the satellite position and satellite clock estimates, but in certain cases, the particular mission could benefit from more accurate navigation solutions. If the mission is not time-critical, delaying the use of the navigation solutions may be acceptable until the postfit precise ephemerides are available. In this case, significantly better results may be expected.

With a precise ephemerides, static absolute position solutions can achieve sub-meter repeatability.[1,2] Meter-level navigation solutions have been demonstrated by postprocessing L_1 observations with postfit precise ephemerides, clock estimates, and an ionospheric model.[3] Applications where precise absolute navigations would be of interest include cases where differential or relative data are not available, or where the track of a moving vehicle or ship is desired at remote locations far from other sites.

In the operational environment, the PPS navigation solutions will be obtained from a user in the field. Presumably, these solutions would be obtained with a receiver that can correct for the effects of Selective Availability (SA) and AntiSpoofing (AS). AS encrypts and SA corrupts the Global Positioning System (GPS) signals, making the precise signal and the full accuracy of the broadcast ephemerides accessible to authorized users only. These receivers can display the navigation solution in real time, but the field-corrected satellite ephemerides and the SA-corrected pseudorange and phase observations are classified and therefore are not available to the user. The PPS position solutions are unclassified and can be recorded in the field along with the GPS time and the satellites contributing to the solution. Even though the original observations are lost, this information is enough to allow the PPS solutions to be improved at a later time with the postfit precise ephemerides.

METHOD

For this description of the method, it will be assumed that the GPS time and the PPS solutions to be improved are given, as are the receiver type and the details of the navigation algorithm it used. The algorithm information may be needed to establish which satellites, of those in view, produced the particular navigation solution. Alternately, the field receiver may be able to supply the satellite pseudo random noise (PRN) numbers that were tracked. To compute the difference between the two ephemerides, an independent source of the SA-corrected broadcast ephemerides and the Defense Mapping Agency (DMA) precise ephemerides and clock estimates are required. Finally, for testing

purposes, two-frequency, SA-corrected, pseudorange and phase observations from a typical receiver need to be added to the requirements.

STANDARD POSITIONING SERVICE (SPS) SOLUTIONS

The form of the observation equations that produces the SPS navigation solution in the field receiver can be reconstructed as in Equation (1). The original observation vector at time t_k is denoted by O_k. The ranges computed from the satellite ephemerides and the estimate of the current state $\tilde{X}_k$ are placed in the C_{bk} vector. The inherently nonlinear problem is then linearized by writing the observation vector equal to the first two terms of the Taylor series expansion for C_{bk}.

$$O_k = C_{bk} + \frac{\partial C_{bk}}{\partial X_k} \Delta X_{bk} + \epsilon_{bk} \tag{1}$$

The last term, ϵ_{bk}, represents the contributions from the terms that are ignored, plus noise. The solution to Equation (1) is ΔX_{bk}, which is found by least squares in the usual way, as indicated in Equation (2). The W is the observation weight matrix that may be incorporated into the formulation.

$$\Delta X_{bk} = (A^T W A)^{-1} A^T W (O_k - C_{bk}) \tag{2}$$

The matrix A in Equation (2) represents the matrix of partials written as $\frac{\partial C_{bk}}{\partial X_k}$ in Equation (1). From this result, the SPS state estimate $\hat{X}_{bk}^{SPS}$ can be found by adding the state update to the current state estimate: $\hat{X}_{bk}^{SPS} = \tilde{X}_k + \Delta X_{bk}$. It is worth noting that if the precise ephemerides were available in the field along with the broadcast ephemerides, the same observation vector, O_k, could have been used with either of these ephemerides to produce a position solution.

PPS SOLUTIONS

The PPS user forms and solves the same sort of equations as the SPS user. The difference is that corrections for SA are included. AS will not be discussed since it has no direct effect on the PAN algorithm. AS may deny certain classes of receivers access to two-frequency observations and the ionospheric correction. It also denies the use of the precision available from P-code observations. The PPS user is assumed able to recover the two-frequency P-code and use it in the observation vector.

The PPS receiver applies the dither corrections to the pseudorange and phase observations. When applied, the original observation vector, O_k, is changed to $\acute{O}_k$. The receiver also applies the epsilon corrections to the broadcast ephemerides messages. The corrections appear in the satellite position part of the C_{bk} vector and change it to the $\acute{C}_{bk}$ vector. Note that both of these SA-corrected vectors are required for a field PPS solution, but neither can be saved for later use. From there, the

route to the PPS solutions proceeds in the same fashion as for the SPS. The PPS observation equation is the same as Equation (1) except that the corrected vectors are used, as shown in Equation (3).

$$\acute{O}_k = \acute{C}_{bk} + \frac{\partial \acute{C}_{bk}}{\partial X_k} \Delta \acute{X}_{bk} + \acute{\epsilon}_{bk} \tag{3}$$

When Equation (3) is solved by least squares in the same manner as before, the PPS state vector $\hat{X}_{bk}^{PPS}$ is found from the sum: $\hat{X}_{bk}^{PPS} = \tilde{X}_k + \Delta \acute{X}_{bk}$.

PPS WITH A PRECISE EPHEMERIDES

Suppose that precise ephemerides were available in the field when the PPS solution was computed. The observation equation would be as shown in Equation (4) where the subscript p on C_{pk} denotes that the satellite positions originate from the precise ephemerides. There is no need for an epsilon correction to the postfit precise ephemerides, but the observation vector, on the left, is the same as the dither-corrected vector used in Equation (3).

$$\acute{O}_k = C_{pk} + \frac{\partial C_{pk}}{\partial X_k} \Delta X_{pk} + \epsilon_{pk} \tag{4}$$

Since this observation vector is common to Equations (3) and (4), they can be equated. This is shown in Equation (5).

$$\acute{\epsilon}_{bk} + \acute{C}_{bk} + \frac{\partial \acute{C}_{bk}}{\partial X_k} \Delta \acute{X}_{bk} = C_{pk} + \frac{\partial C_{pk}}{\partial X_k} \Delta X_{pk} + \epsilon_{pk} \tag{5}$$

From Equation (3) the PPS field solution $\hat{X}_{bk}^{PPS}$ is known. Therefore it can be used in Equation (5) in place of the initial estimate $\tilde{X}_k$. New computed vectors are needed to reflect the change in the initial state estimate; these are indicated by the PPS superscript. This substitution does not change the equality as long as the observation vector remains unchanged and the linearity constraint continues to be satisfied. The new form for Equation (5), incorporating the PPS position, is shown in Equation (6).

$$\acute{C}_{bk}^{PPS} + \frac{\partial \acute{C}_{bk}^{PPS}}{\partial X_k} \Delta \acute{X}_{bk} = C_{pk}^{PPS} + \frac{\partial C_{pk}^{PPS}}{\partial X_k} \Delta X_{pk} + \epsilon_{pk}^{PPS} \tag{6}$$

If $\hat{X}_{bk}^{PPS}$ were used instead of $\tilde{X}_k$ in Equation (3), and the system solved, the new state solution would be near zero. This result is usually called the *adjusted O minus C* and reflects the level of observation noise and residual unmodeled effects. Therefore the second term from the left in Equation (6) can

be neglected, because the state vector $\Delta \acute{X}_{bk}$ is approximately zero. When this is the case, Equation (6) reduces to a simpler form shown in Equation (7).

$$\acute{C}_{bk}^{PPS} \approx C_{pk}^{PPS} + \frac{\partial C_{pk}^{PPS}}{\partial X_k} \Delta X_{pk} + \epsilon_{pk}^{PPS} \tag{7}$$

Equation (7) can be solved by least squares for ΔX_{pk} in an expression like Equation (2).

$$\Delta X_{pk} = (A^T W A)^{-1} A^T W (\acute{C}_{bk}^{PPS} - C_{pk}^{PPS}) \tag{8}$$

Then the improved state, with the quality of the postfit precise ephemerides, is $\hat{X}_{pk}$ and is found from the sum: $\hat{X}_{pk} = \hat{X}_{bk}^{PPS} + \Delta X_{pk}$. This is the PAN solution. The foregoing argument is equivalent to noting in Equation (3) that when $\Delta \acute{X}_{bk}$ is zero, the vector $\acute{C}_{bk}$, plus some noise ϵ_{bk}, is equal to the observation vector. Therefore it is possible to approximately recreate the lost observations from knowledge of the satellite ephemerides and the solution vector $\hat{X}_{bk}^{PPS}$.[4]

PAN EVALUATION

PAN assumes that PPS field solutions exist, so the first task on the way to verification of the method was to generate simulated PPS solutions from GPS observations already on hand. This required that a navigation algorithm be developed and tested. The formulation for this algorithm is attached as Appendix A. The solutions obtained from the navigation algorithm were intended to substitute for the PPS field solutions that are the starting point for the PAN algorithm. The navigation solutions require GPS observations, and two sources of existing data were available as described in the following paragraphs.

DMA provided one data set for one week of observations at static site 85401 in March 1995. An Ashtech Z12 receiver was used. The data interval was 30 sec and both SA-uncorrected and SA-corrected observations were provided. For the PAN application, the SA-corrected data were used in the navigation algorithm to simulate PPS solutions from a field site. Coordinates for this site were provided with the data, but absolute position solutions were also performed on three of the days as a check. The site documentation is included as Appendix B.

The second set of observations were selected from the Drive-By experiment performed at the Naval Surface Warfare Center, Dahlgren Division (NSWCDD), Dahlgren, Virginia, in February 1994. Four Trimble 4000 SSE receivers collected 1-sec data simultaneously for tests of Remondi's on-the-fly (OTF) algorithm.[5] Two of these receivers were at fixed sites and two traveled several laps around a circuit on the naval base with antennas attached to the roofs of two vehicles. The data sets were given to DMA in May 1995 so that the SA effects could be removed in the DMA Data Correction Facility (DCF). The SA-corrected data are classified, and were processed by the navigation algorithm

in a classified facility. The resulting unclassified, simulated PPS solutions were compared with the OTF results, which represented the true vehicle track with an estimated error of a few centimeters.

STATIC SITE RESULTS

The true absolute position for 85401 was obtained relative to a primary control station, USAF3 1988. The errors in the relative positioning are given as ±0.02 m in each component, while the absolute error in USAF3 is given as ±1 m in each component with respect to the World Geodetic System (WGS84) datum. These coordinates are used throughout this section as the true position for 85401.

The SA-corrected observations and broadcast ephemerides were processed with the navigation algorithm to obtain the simulated PPS field solutions. The PPS solutions were then used with the DMA precise ephemerides and clock estimates to perform the PAN solutions at each PPS epoch. The daily PAN averages showed a consistent 1.5- to 2.0-m offset in the north and −1.0 m east, compared with the truth (PAN - Truth). Since this disagreement may be have been due to small errors in the truth, three days' data were processed with the DMA absolute positioning program GASP.[6] The results from GASP using the SA-corrected broadcast ephemerides are shown in Table 1; the results using the precise ephemerides are shown in Table 2. As expected, the consistency between the three days is better with the precise ephemerides. This is quantified by the smaller standard deviations for the latitude, longitude, and height in Table 2.

TABLE 1. GASP SOLUTIONS FOR 85401 WITH SA-CORRECTED BROADCAST EPHEMERIDES

DATE 1995	LAT DELTA (m)	LONG DELTA (m)	EL HGT DELTA (m)	RSS (G)* (m)	X DELTA (m)	Y DELTA (m)	Z DELTA (m)	RSS (C)** (m)	RMS (cm)	NO. OF OBSV	% REJEC-TED
072	0.081	-0.131	1.306	1.315	-0.135	-0.969	0.879	1.315	4.900	8060	1.0
073	-0.867	-2.065	1.686	2.803	-2.072	-1.850	0.376	2.803	9.100	7799	3.0
075	0.997	-1.373	-1.212	2.085	-1.367	1.575	0.022	2.085	4.500	8097	1.0
MEAN:	0.070	-1.189	0.593	2.068	-1.191	-0.415	0.426	2.068	6.167		
STD:	0.932	0.980	1.575	0.744	0.981	1.778	0.431	0.744			
STDM:	0.538	0.566	0.909		0.566	1.027	0.249				
TOTAL NUMBER OF DAYS PROCESSED: 3											

* Geodetic

** Coordinates

The mean solutions from Table 2 move the station location 0.3 m north and −1.03 m east. If both of these changes were adopted, the east PAN position error would be nearly zero, but a 1.5-m disagreement would remain in the north component. The cause of this north error is unresolved at this writing. The average PPS and PAN navigation solutions for each day are listed in Tables 3 and 4. Table 3 includes the total number of 30-sec epochs processed on each day.

TABLE 2. GASP SOLUTIONS FOR 85401 WITH PRECISE EPHEMERIDES

DATE 1995	LAT DELTA (m)	LONG DELTA (m)	EL HGT DELTA (m)	RSS (G)* (m)	X DELTA (m)	Y DELTA (m)	Z DELTA (m)	RSS (C)** (m)	RMS (cm)	NO. OF OBSV	% REJEC-TED
072	0.184	-1.049	-0.010	1.065	-1.049	0.127	0.137	1.065	4.200	8028	1.0
073	0.432	-1.028	-0.609	1.270	-1.025	0.749	-0.042	1.270	4.300	8038	0.0
075	0.284	-1.025	-0.709	1.279	-1.023	0.735	-0.220	1.279	4.100	8015	1.0
MEAN:	0.300	-1.034	-0.443	1.205	-1.032	0.537	0.042	1.205	4.200		
STD:	0.125	0.013	0.378	0.121	0.015	0.355	0.179	0.121			
STDM:	0.072	0.008	0.218		0.008	0.205	0.103				
TOTAL NUMBER OF DAYS PROCESSED: 3											

* Geodetic
** Coordinates

TABLE 3. DAILY STATIC PPS WEIGHTED MEANS (μM) AND STANDARD DEVIATIONS (σM)

	071		072		073		074		075		076		077	
	μ	σ	μ	σ	μ	σ	μ	σ	μ	σ	μ	σ	μ	σ
E*	-0.55	2.27	-0.44	2.53	-0.90	2.89	1.07	1.68	-0.42	2.21	-1.87	8.69	1.01	1.81
N**	-0.28	2.99	0.23	3.28	0.52	5.12	0.80	4.29	0.56	3.12	1.45	8.07	-0.52	2.75
U†	1.09	6.52	-0.60	9.35	1.14	8.86	2.37	5.65	1.80	7.88	-3.38	17.26	0.62	4.95
S††	2393		2833		2833		1652		2833		2826		719	

* East Component
** North Component
† Vertical Component
†† Number of 30-sec observations processed each day

TABLE 4. DAILY STATIC PAN WEIGHTED MEANS (μM) AND STANDARD DEVIATIONS (σM)

	071		072		073		074		075		076		077	
	μ	σ	μ	σ	μ	σ	μ	σ	μ	σ	μ	σ	μ	σ
E*	-0.78	0.66	-0.93	0.27	-0.92	1.88	-0.90	0.62	-0.85	0.66	-0.66	2.04	-1.12	0.56
N**	1.82	1.27	1.77	1.27	1.87	1.36	1.79	1.23	1.88	1.30	1.90	4.01	1.82	1.34
U†	0.09	1.88	0.34	1.94	0.17	3.21	0.70	1.80	0.19	1.85	-0.41	8.29	0.42	1.75

* East Component
** North Component
† Vertical Component

Figure 1 shows a plot of the Geometric Dilution Of Precision (GDOP) for the navigation solutions obtained for 85401. The elevation cutoff angle was set at 15 deg in order to restrict the use of low elevation satellites and improve the quality of the solutions. The receiver tracked all satellites down to 10 deg, but there were frequent jumps in the solutions when data at the lower elevation angles were included. The GDOP peaks at over 600 during a short span of the day. The satellite elevation angles during this period are plotted in Figure 2. Just four satellites are in view above 15 deg for about 2300 sec beginning at about 142,200 sec.

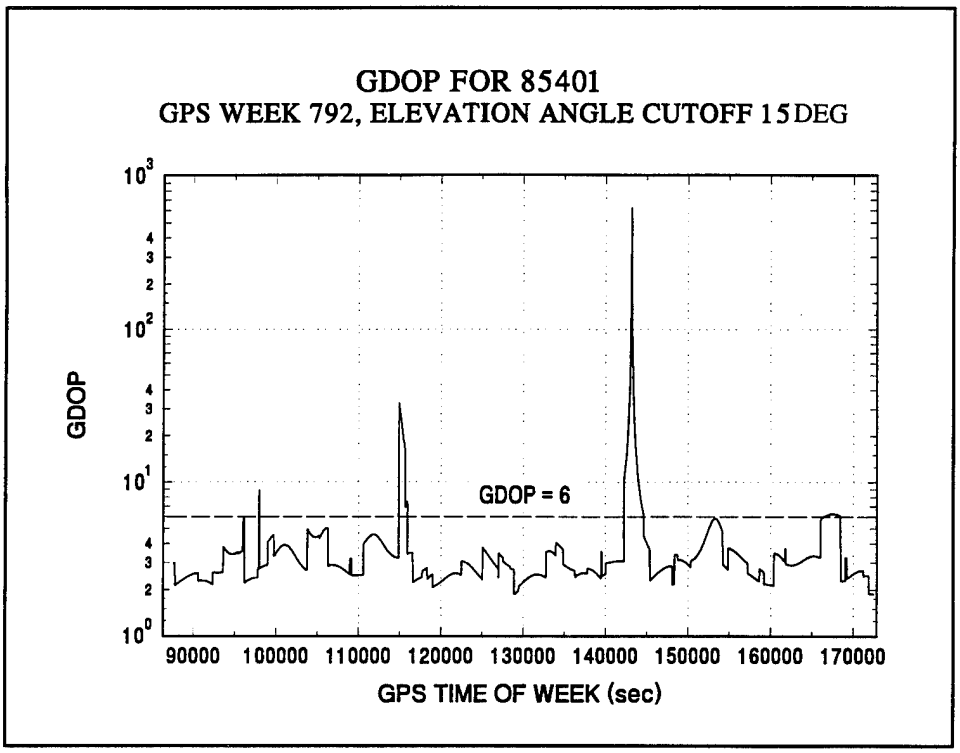

FIGURE 1. GDOP AT 85401 WITH A 15-DEG ELEVATION CUTOFF

The adjusted observed-minus-computed residuals are the differences between the observations and the computed values after the current state solution is substituted for the predicted state. The least squares solution minimizes the square of the residuals; therefore, the adjusted residuals have zero mean. The RMS of the pseudorange residuals for the PPS and PAN solutions for site 85401 and day 072 are plotted in Figure 3. The jumps in the residuals are due to new satellites being included in the solution or satellites dropping out of the solution. Only four satellites were included in the solution during periods where the adjusted residual is zero. Since the two curves are similar, the source of the unmodeled residuals must be common to both solutions.

Figures 4 to 17 illustrate the differences between the navigation solutions and the true position for 85401 on each of the seven days. The seven even-numbered figures show the PPS solutions, and the odd-numbered figures show the PAN solutions. The improvement due to the precise ephemerides is evident in the PAN solutions. The large variations that remain in the solutions are primarily associated with high GDOP periods.

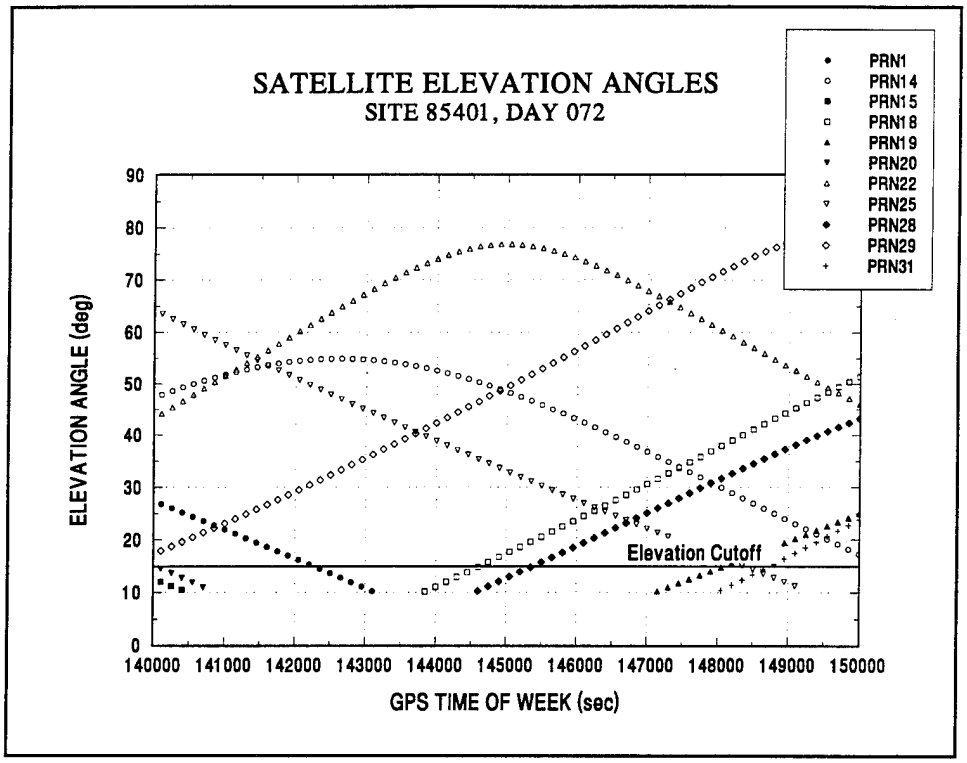

FIGURE 2. SATELLITE ELEVATION ANGLES DURING PERIOD OF HIGH GDOP

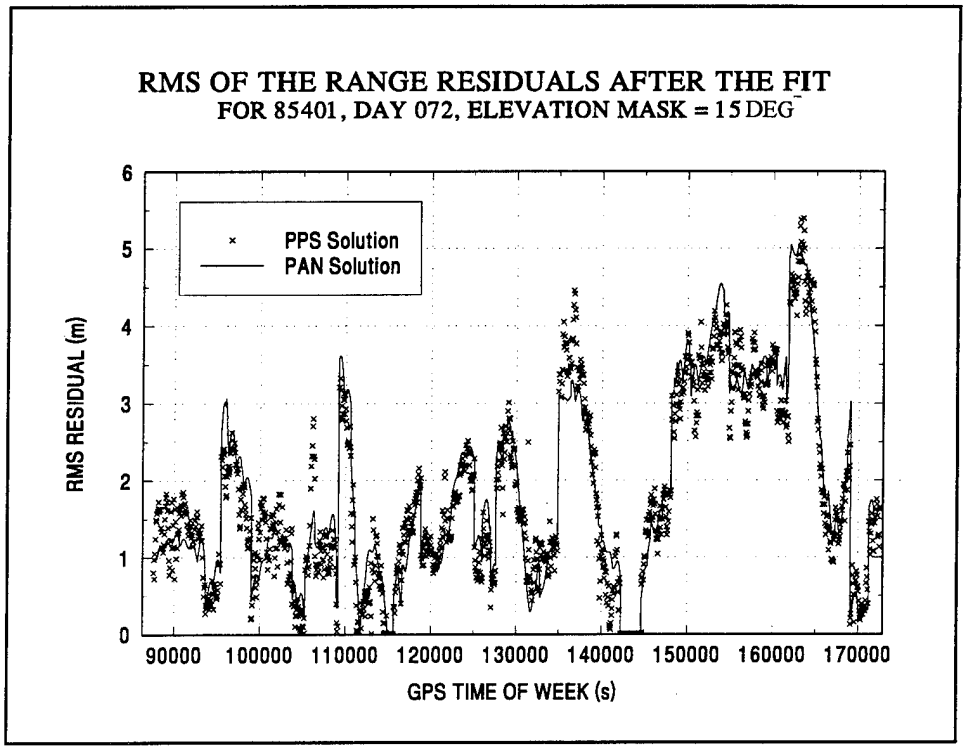

FIGURE 3. PSEUDORANGE ADJUSTED RESIDUALS FOR DAY 072

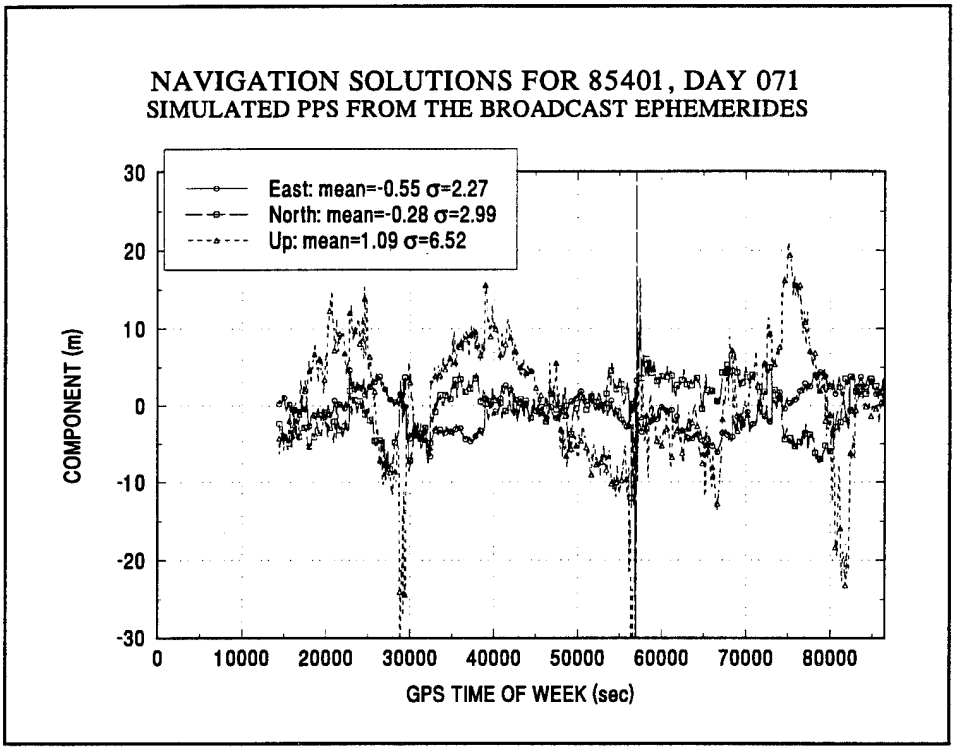

FIGURE 4. PPS SOLUTIONS FOR STATIC SITE 85401, DAY 071

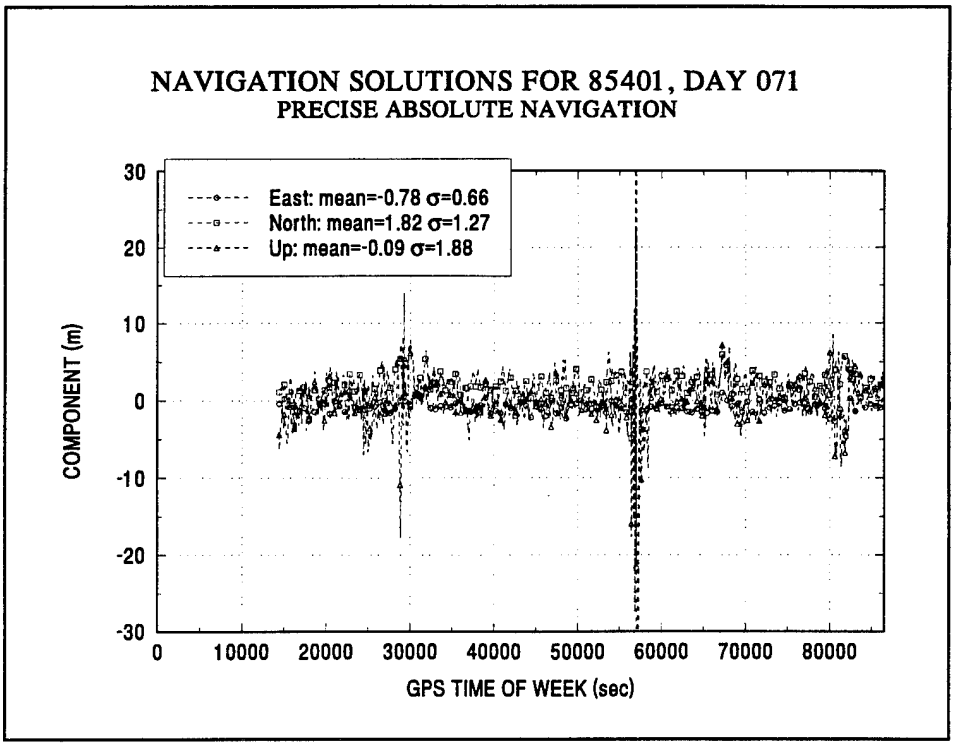

FIGURE 5. PAN SOLUTIONS FOR STATIC SITE 85401, DAY 071

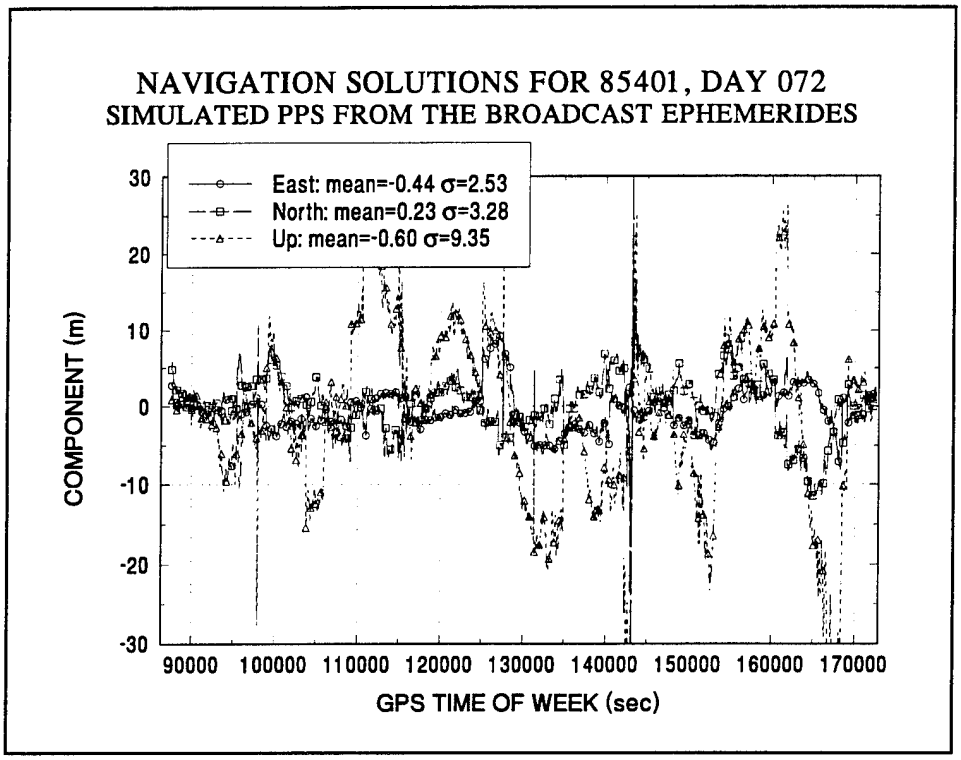

FIGURE 6. PPS SOLUTIONS FOR STATIC SITE 85401, DAY 072

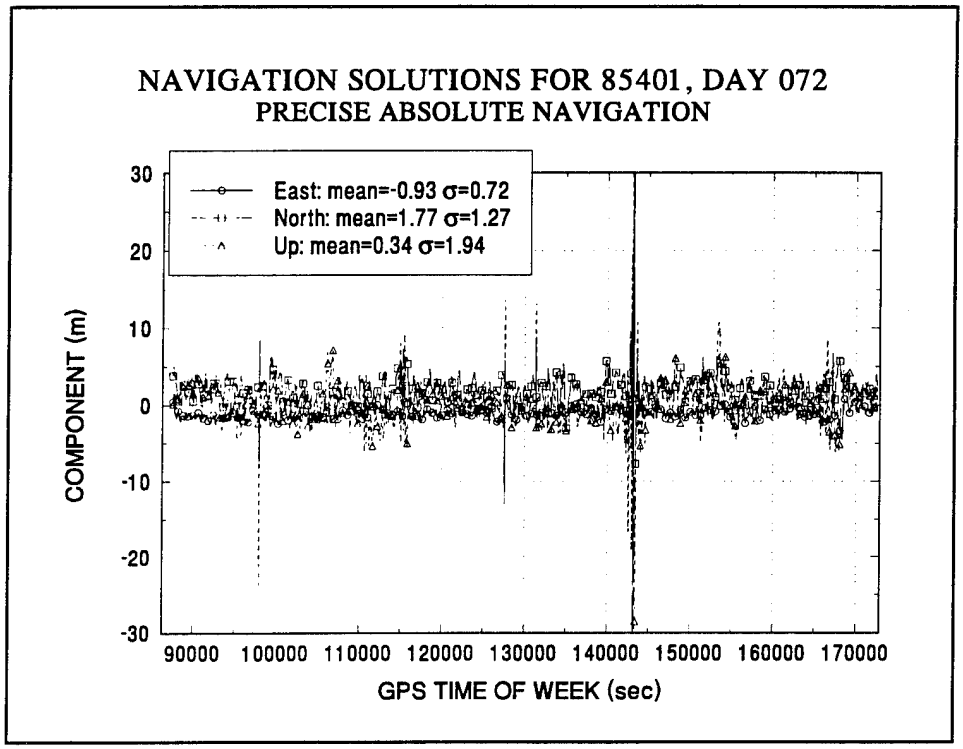

FIGURE 7. PAN SOLUTIONS FOR STATIC SITE 85401, DAY 072

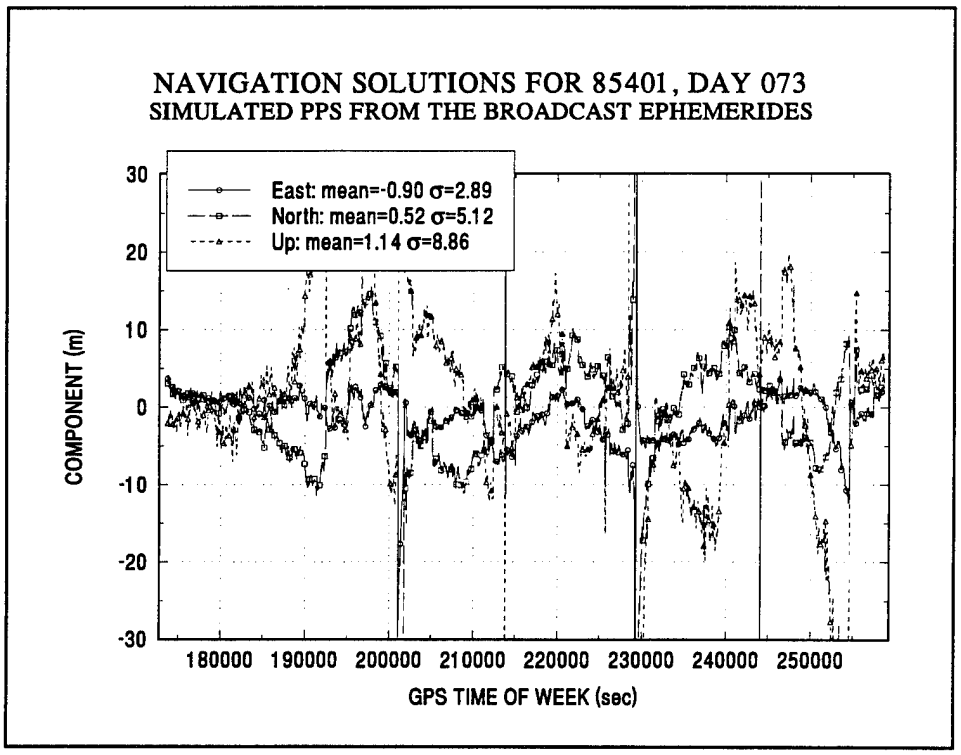

FIGURE 8. PPS SOLUTIONS FOR STATIC SITE 85401, DAY 073

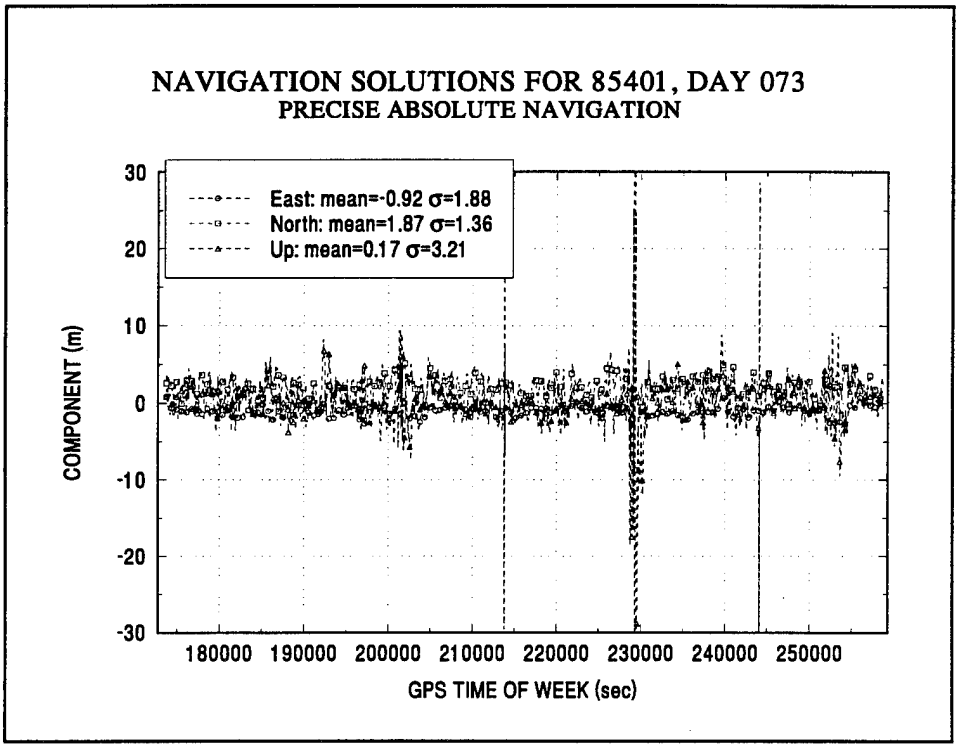

FIGURE 9. PAN SOLUTIONS FOR STATIC SITE 85401, DAY 073

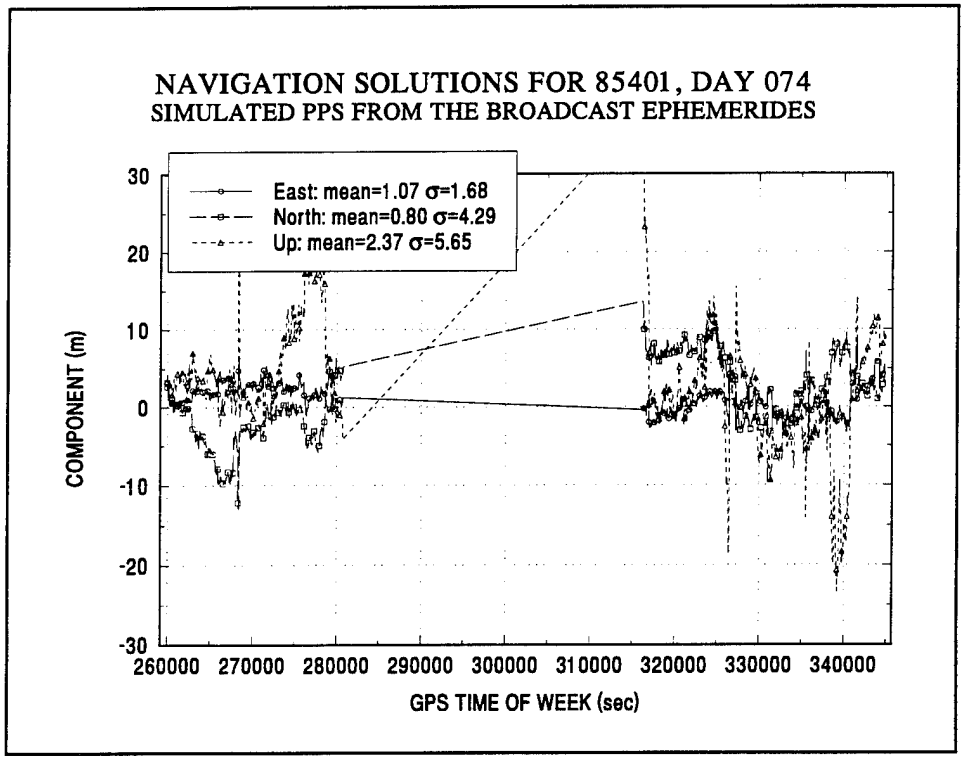

FIGURE 10. PPS SOLUTIONS FOR STATIC SITE 85401, DAY 074

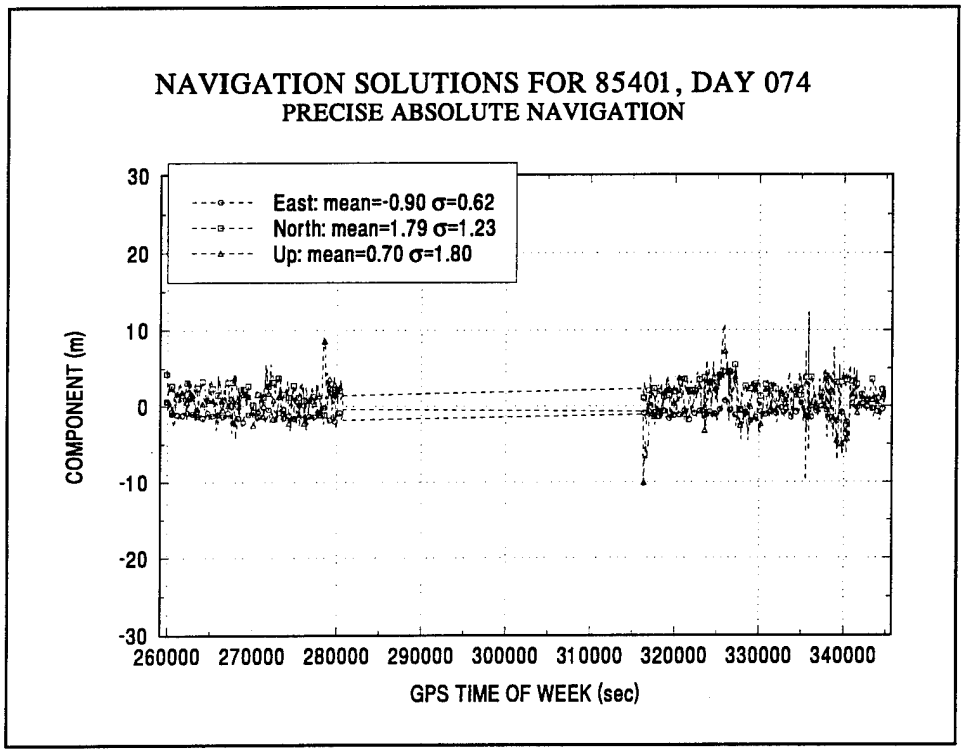

FIGURE 11. PAN SOLUTIONS FOR STATIC SITE 85401, DAY 074

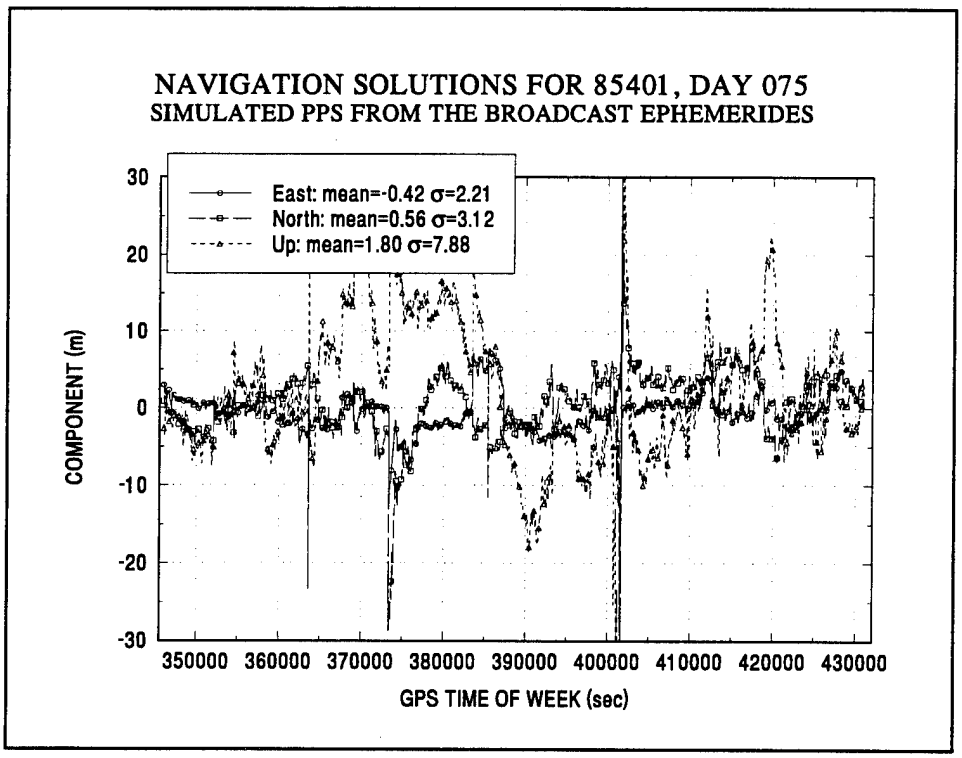

FIGURE 12. PPS SOLUTIONS FOR STATIC SITE 85401, DAY 075

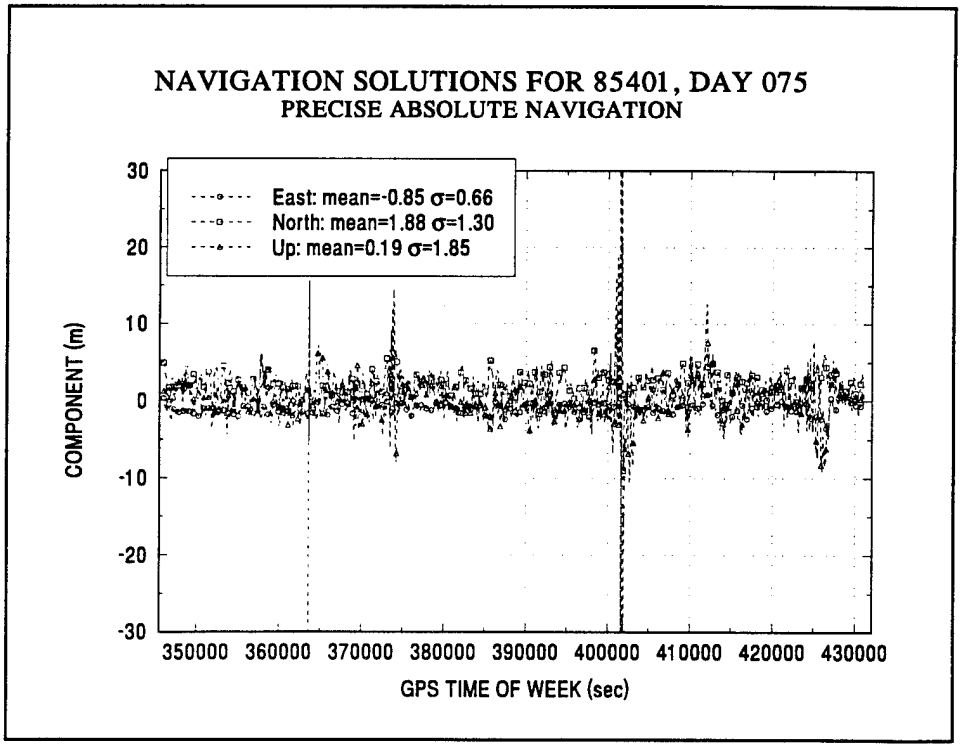

FIGURE 13. PAN SOLUTIONS FOR STATIC SITE 85401, DAY 075

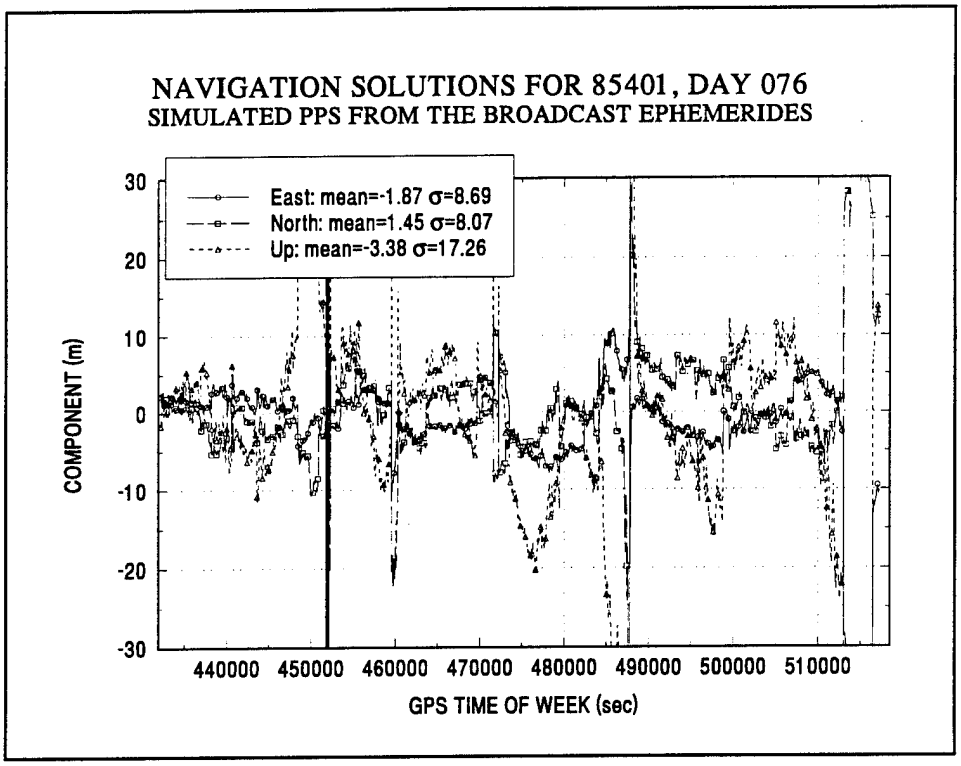

FIGURE 14. PPS SOLUTIONS FOR STATIC SITE 85401, DAY 076

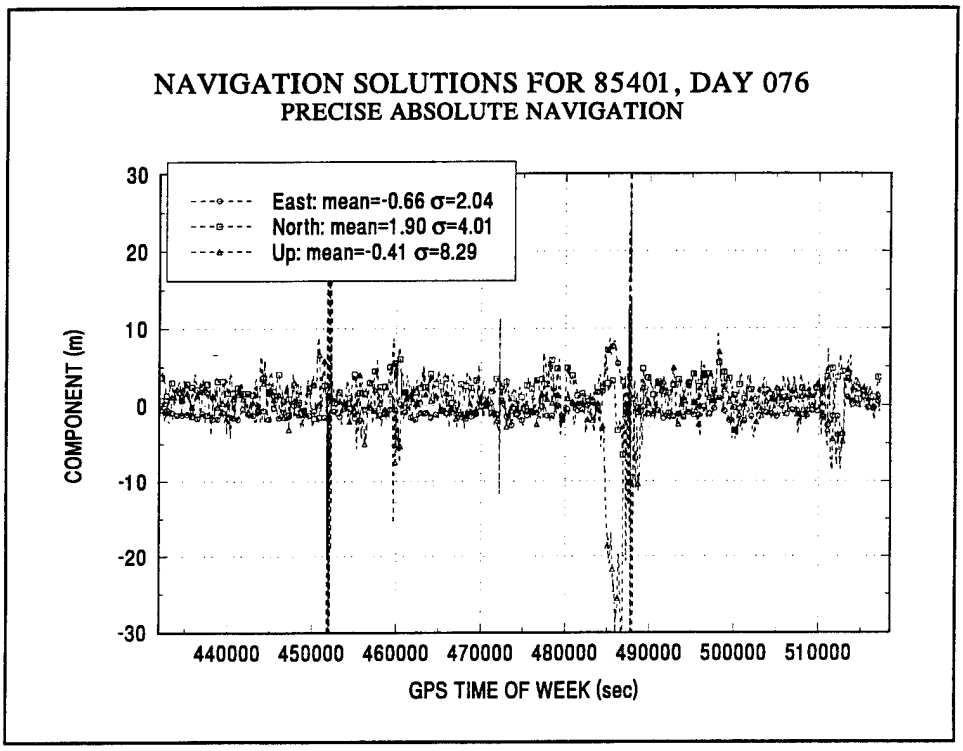

FIGURE 15. PAN SOLUTIONS FOR STATIC SITE 85401, DAY 076

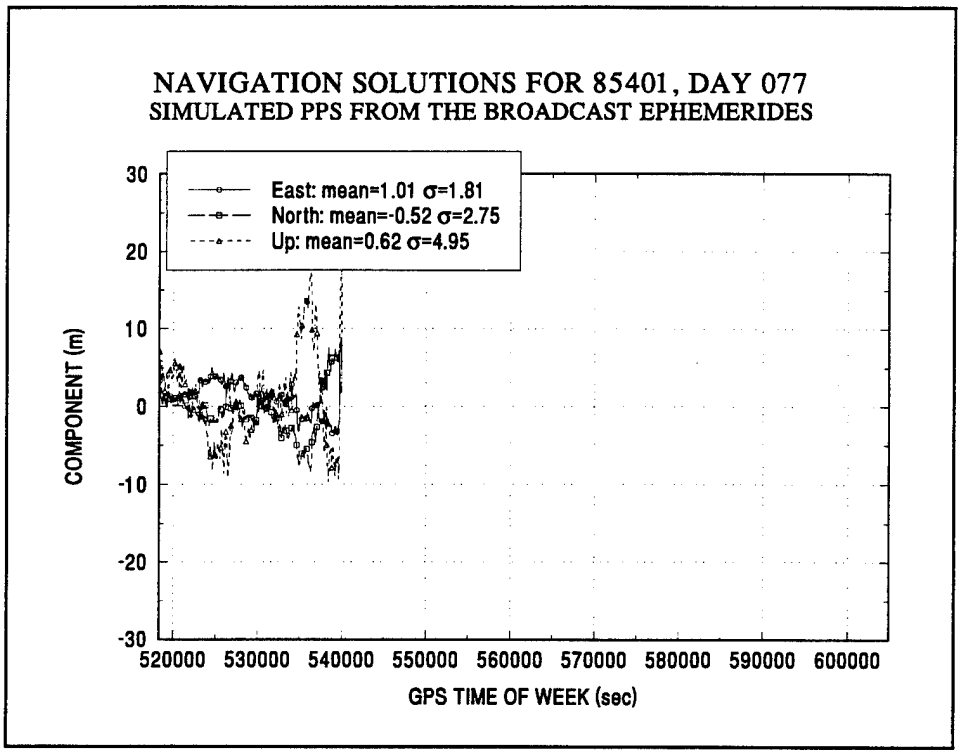

FIGURE 16. PPS SOLUTIONS FOR STATIC SITE 85401, DAY 077

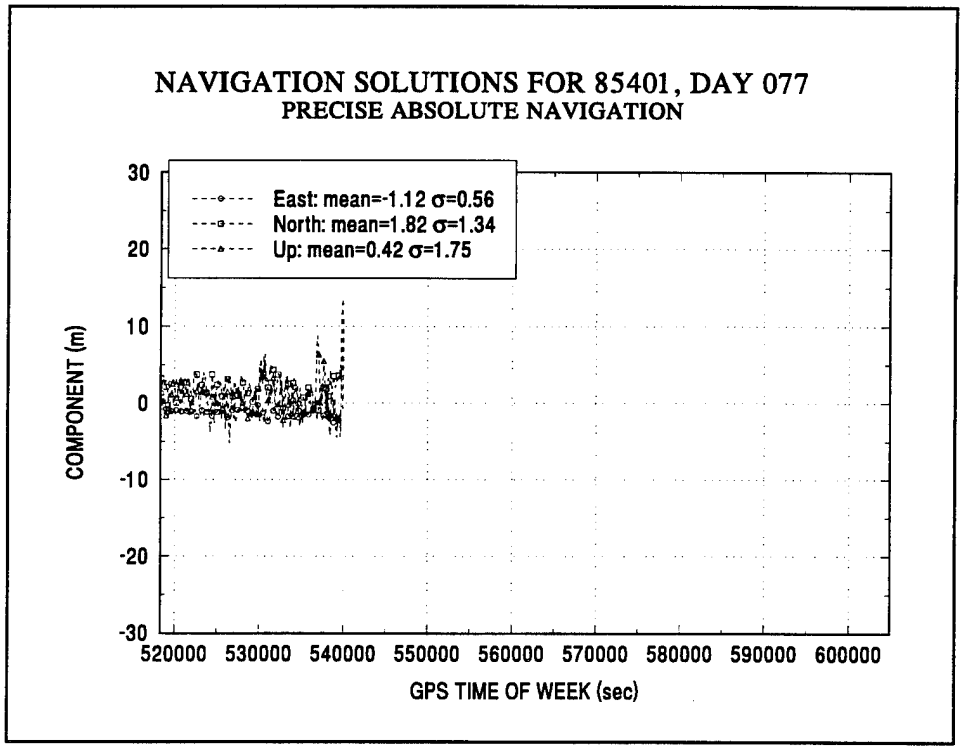

FIGURE 17. PAN SOLUTIONS FOR STATIC SITE 85401, DAY 077

DYNAMIC SITE SOLUTIONS

A map of the roads at NSWCDD on which the dynamic data were collected is shown in Figure 18. The two static site locations are indicated as *MBRE* and *ASTW*. The truth data for the PAN solutions are the OTF results between MBRE and one of the two vehicles that were part of the original test. The path the vehicle took began at the location marked *Turntable*, then followed McVay Road to Dahlgren Road. At the Dahlgren Road intersection, the vehicles made a left turn and followed Dahlgren Road east to the intersection with Caskey Road. A right turn on Caskey Road was followed by two left turns on two secondary roads to return to Dahlgren Road. After the Caskey Road intersection, the vehicle proceeded back to the starting point at the Turntable. Five laps around this circuit are shown in the Figure 19 east vs. north *truth* plot. A second truth plot showing the ellipsoid height vs. east is included as Figure 20. This figure shows that there is little change in height around the circuit.

The PPS solutions for the circuit are shown in Figures 21 and 22. Figure 21 shows the solutions in the east and north components, while Figure 22 shows the east and ellipsoid height components. The corresponding PAN solutions are shown in Figures 23 and 24. For comparison, the SPS solutions are shown in Figures 25 and 26. Note the change in scale in Figure 26. On the east and north scale, the difference between the PPS and PAN solutions are difficult to appreciate, while the improvement in ellipsoid height is easy to see. The area marked DETAIL in Figure 19 is used to illustrate the east and north differences on a smaller scale. For the detail area, the east and north components of the PPS solutions are shown in Figure 27, the east and ellipsoid heights in Figure 28. The corresponding PAN solutions are shown in Figures 29 and 30. A plot of the difference between the PPS solutions and the truth is shown in Figure 31. Each differenced component is plotted separately vs. GPS time of week. The corresponding PAN solutions are shown in Figure 32. A table summarizing the differences is included as Table 5.

DIFFERENTIAL CORRECTIONS

Early in the development of PAN, it was thought that the SPS dynamic vehicle solutions obtained during the Dahlgren vehicle test, described earlier, could be made to simulate the PPS solutions. These data were obtained by four Trimble 4000SE receivers. These are unkeyed receivers, but are capable of recording two-frequency pseudorange and phase data even when AS is operating. Since these receivers are primarily used for kinematic positioning, the SA effects are of little importance to the user. In the case of navigation, the SA dither and radial epsilon errors could be substantially reduced by computing range corrections. This technique was expected to perform an adequate dither correction without resorting to formal SA removal in the DCF. The range corrections were to be computed from static sites whose position was known. These would then be transferred to the dynamic sites during postprocessing.

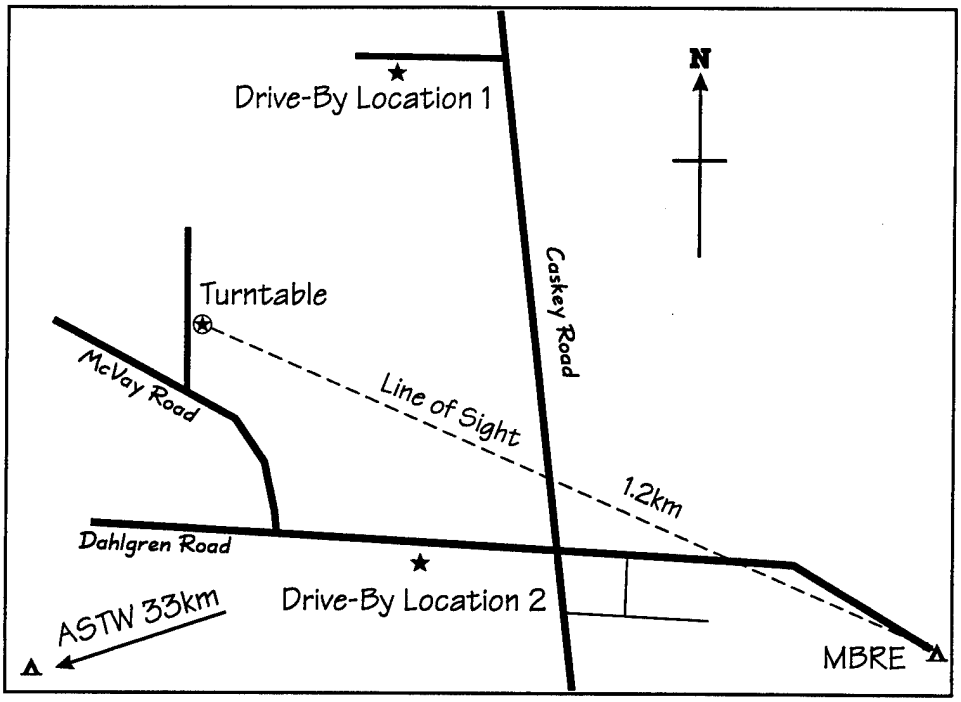

FIGURE 18. MAP SHOWING ROUTE OF VEHICLE AROUND DAHLGREN CIRCUIT

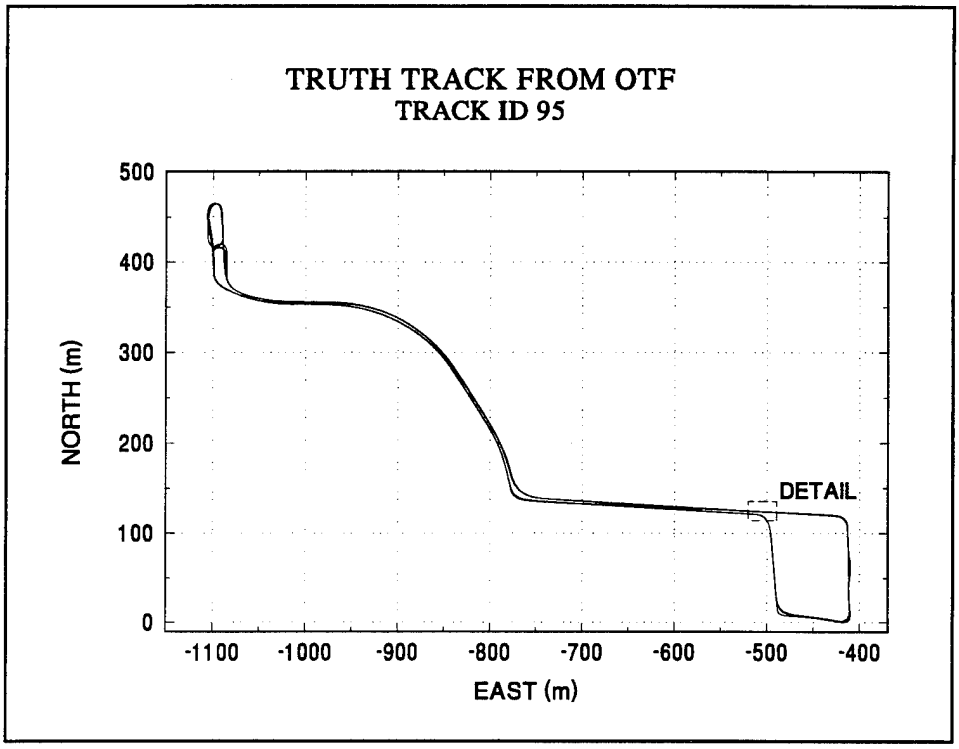

FIGURE 19. TRUTH TRACK AROUND VEHICLE CIRCUIT CORRESPONDING TO FIGURE 18

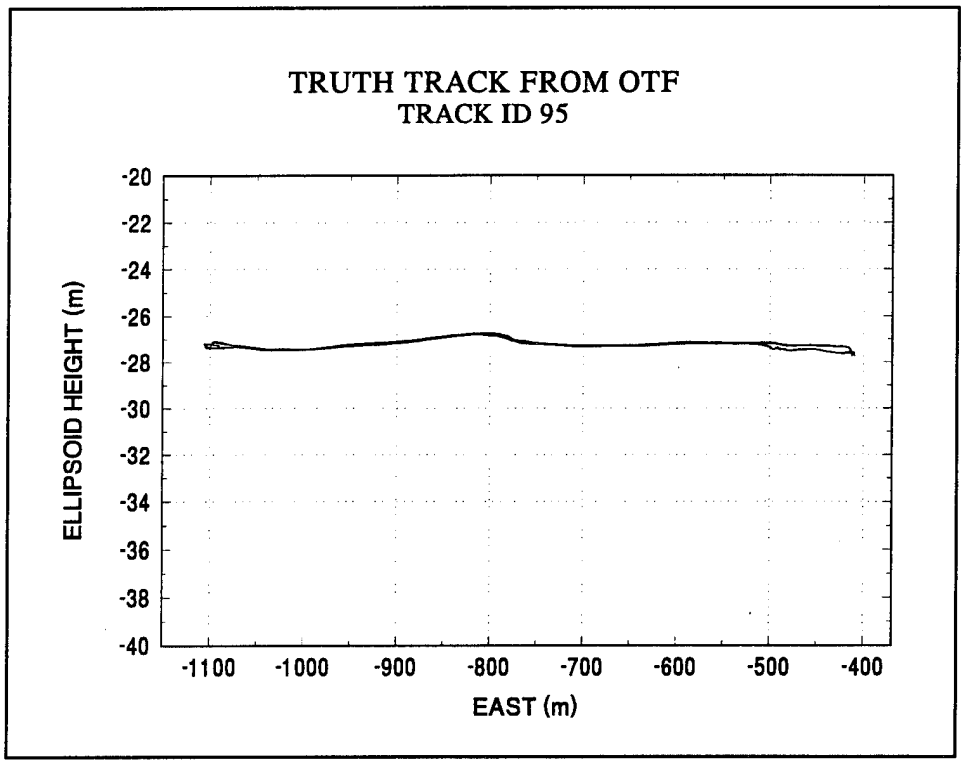

FIGURE 20. TRUTH TRACK CORRESPONDING TO FIGURE 18 SHOWING ELLIPSOID HEIGHT VARIATION

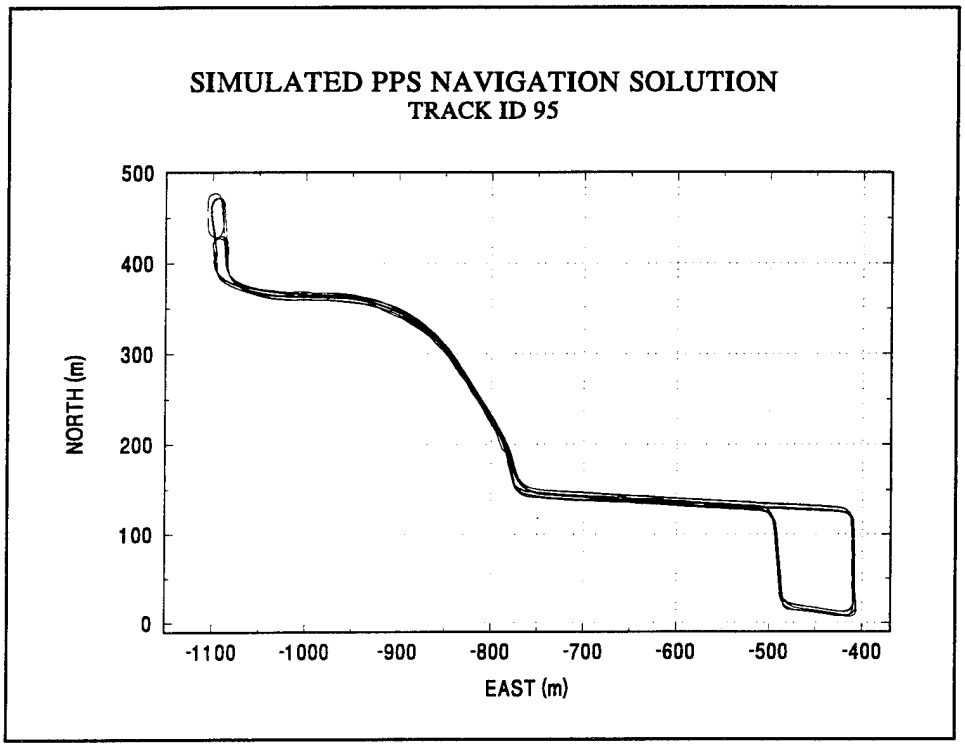

FIGURE 21. PPS TRACK AROUND VEHICLE CIRCUIT CORRESPONDING TO FIGURE 19

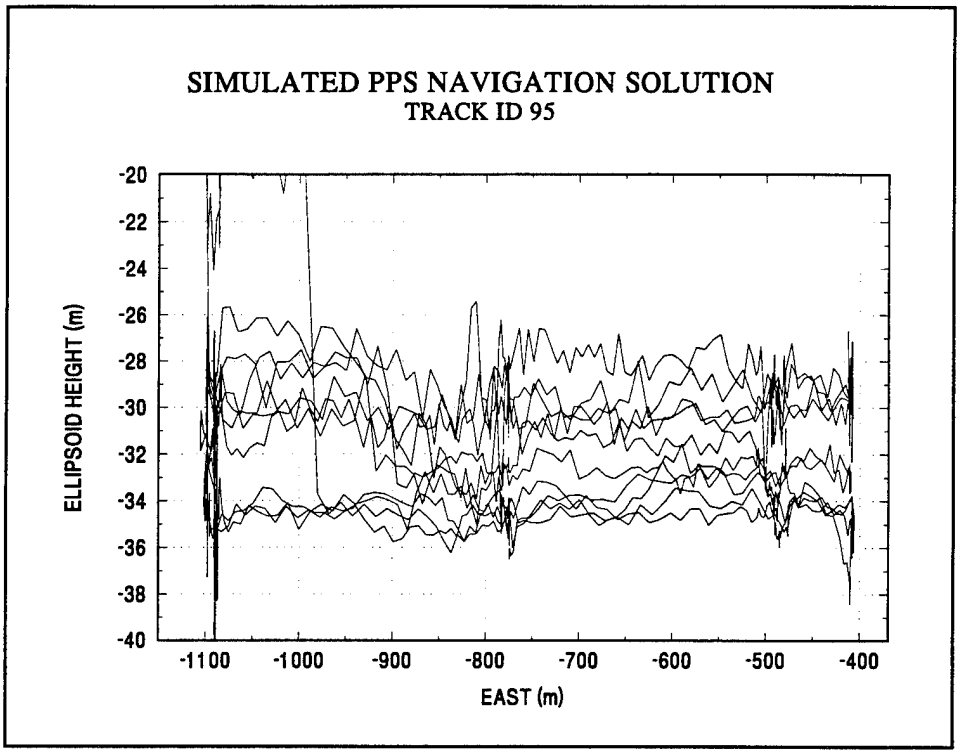

FIGURE 22. PPS TRACK CORRESPONDING TO FIGURE 20 SHOWING ELLIPSOID HEIGHT VARIATION

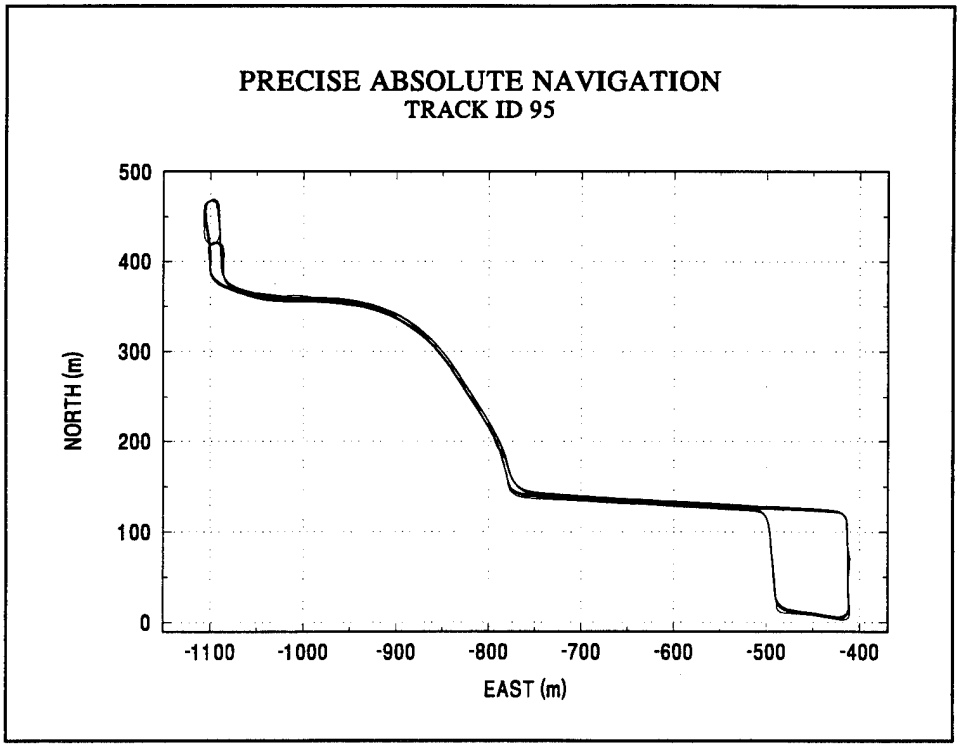

FIGURE 23. PAN TRACK AROUND VEHICLE CIRCUIT CORRESPONDING TO FIGURE 19

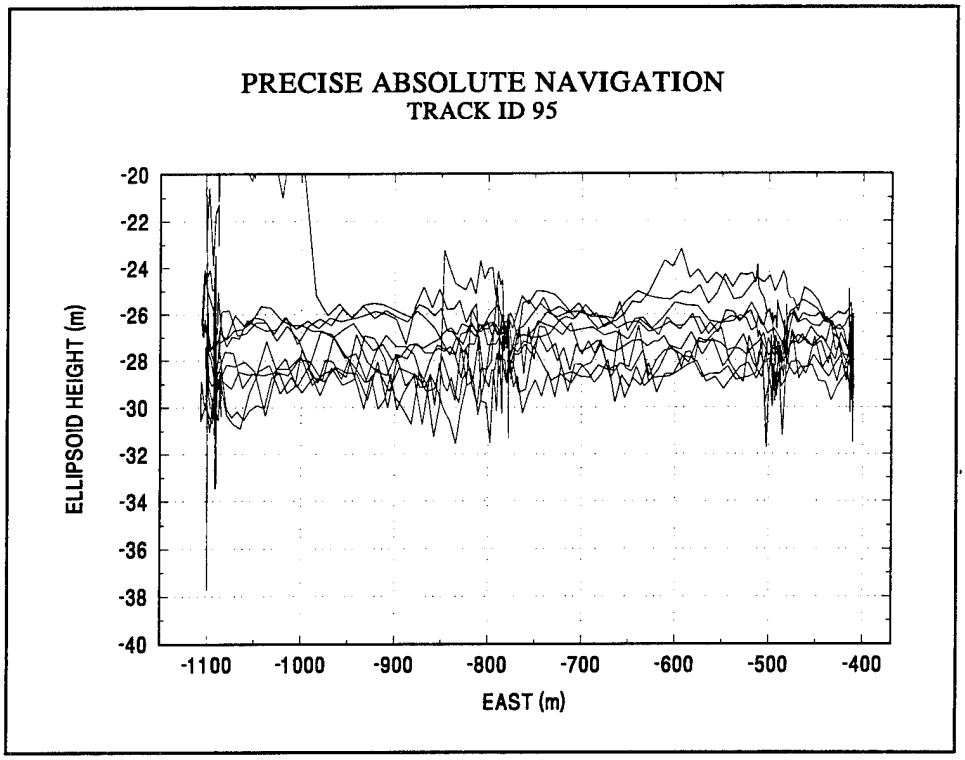

FIGURE 24. PAN TRACK CORRESPONDING TO FIGURE 20 SHOWING ELLIPSOID HEIGHT VARIATION

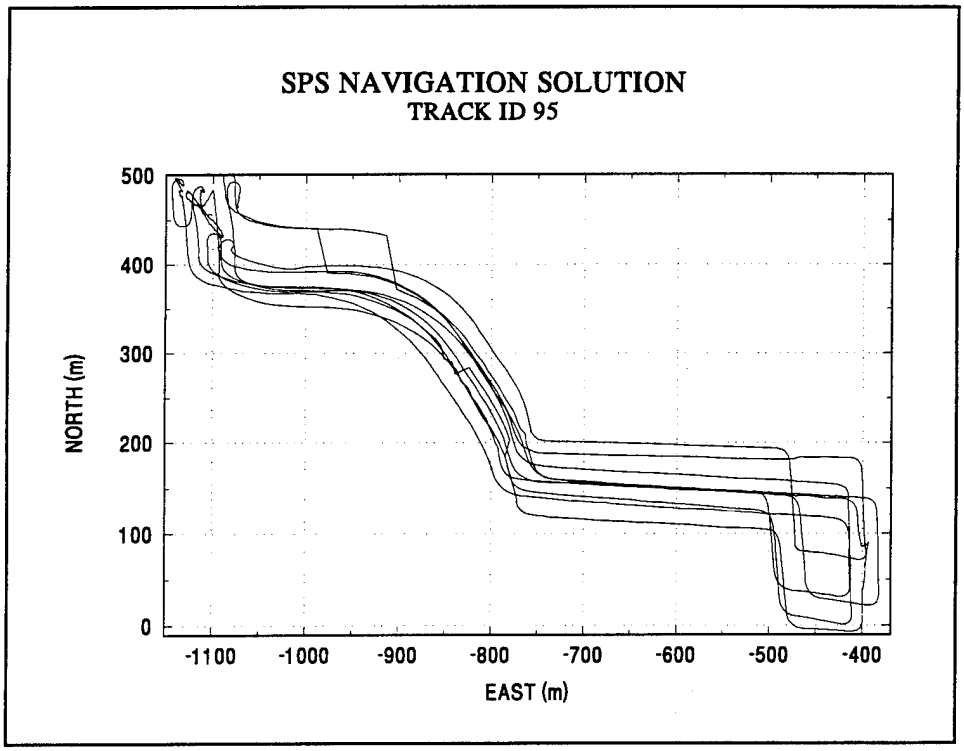

FIGURE 25. SPS TRACK AROUND VEHICLE CIRCUIT CORRESPONDING TO FIGURE 19

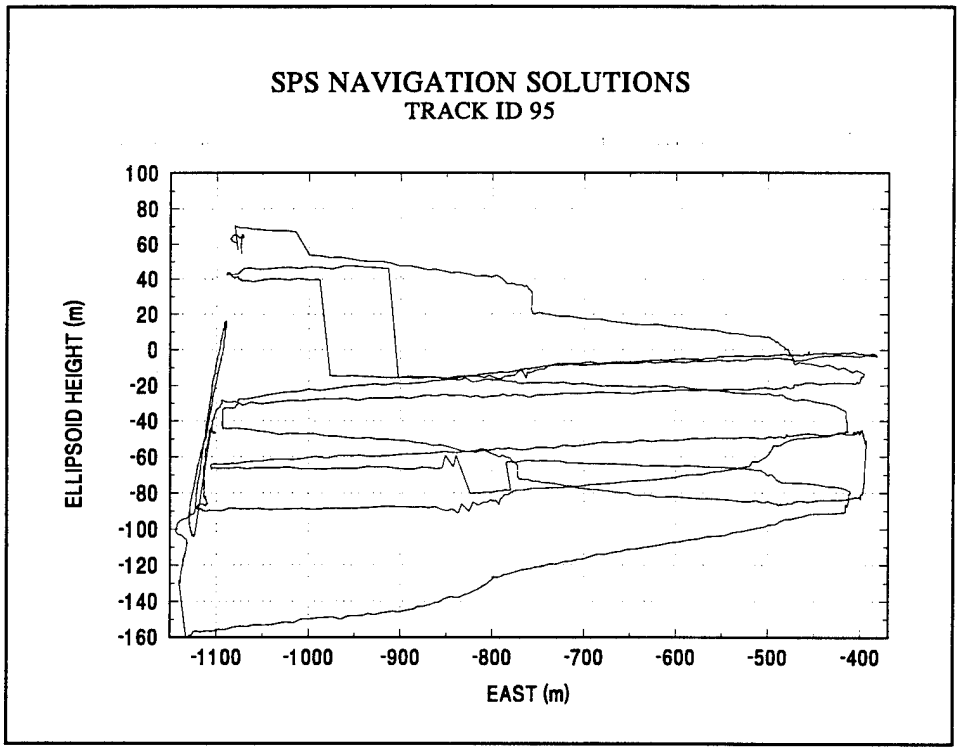

FIGURE 26. SPS TRACK CORRESPONDING TO FIGURE 19 SHOWING ELLIPSOID HEIGHT VARIATION

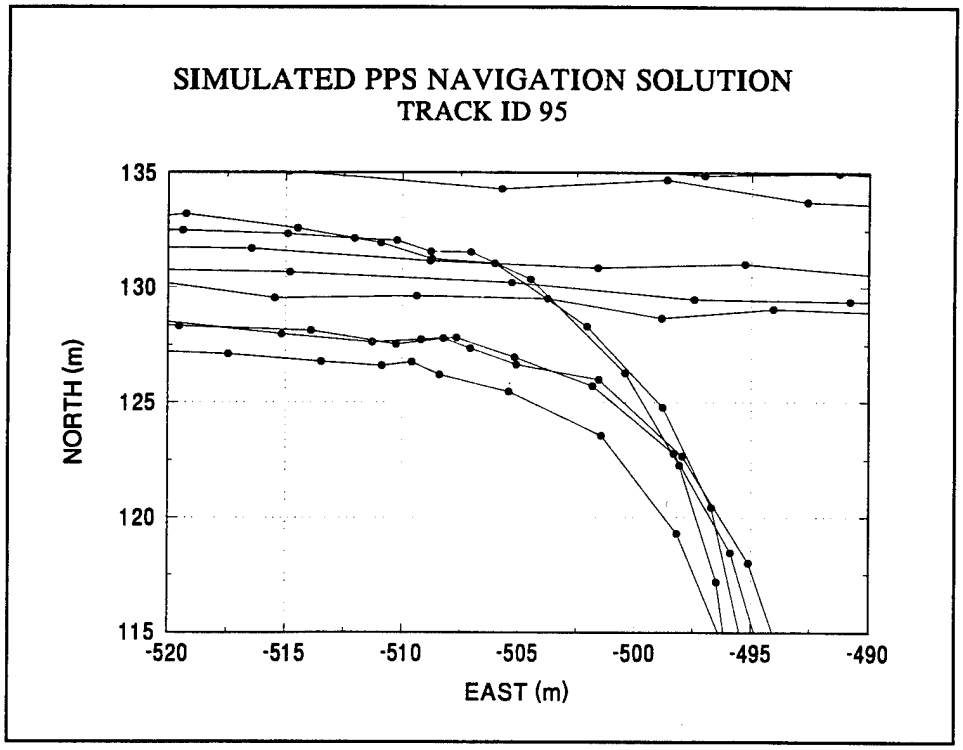

FIGURE 27. PPS TRACK AROUND VEHICLE CIRCUIT CORRESPONDING TO THE DETAIL IN FIGURE 19

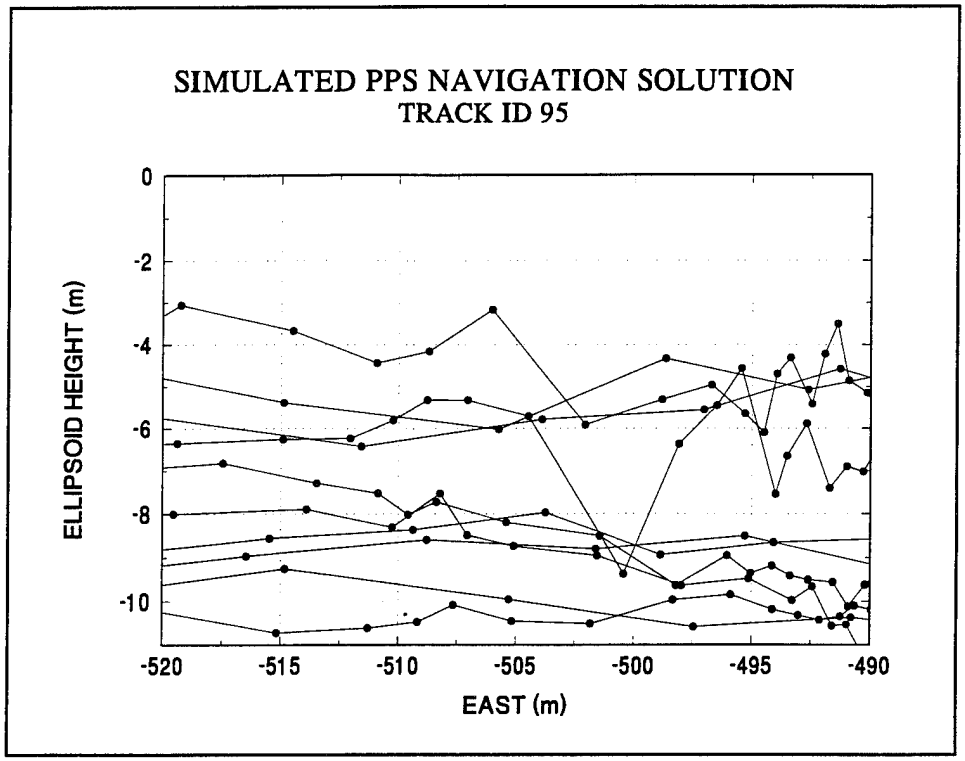

FIGURE 28. PPS TRACK CORRESPONDING TO DETAIL IN FIGURE 19 SHOWING ELLIPSOID HEIGHT VARIATION

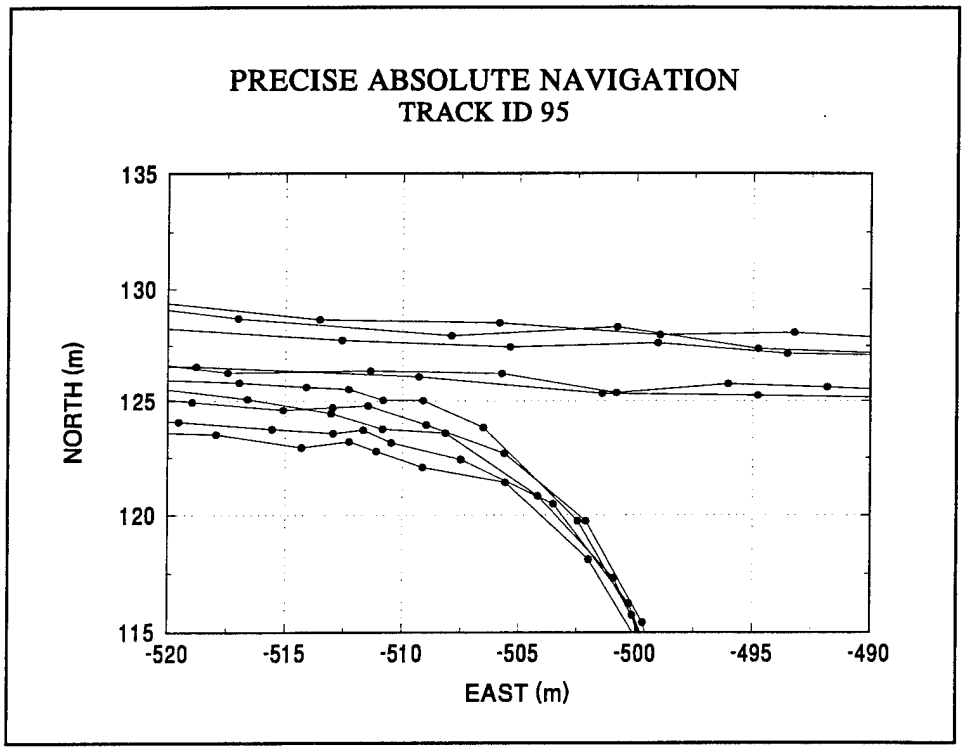

FIGURE 29. PAN TRACK AROUND VEHICLE CIRCUIT CORRESPONDING TO DETAIL IN FIGURE 19

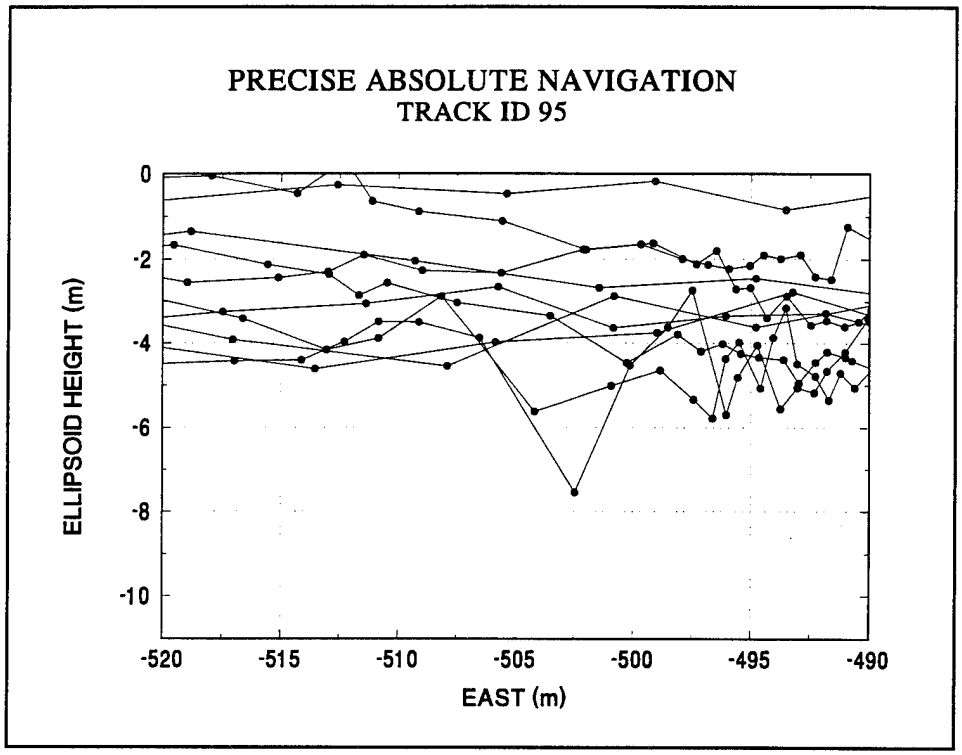

FIGURE 30. PAN TRACK CORRESPONDING TO DETAIL IN FIGURE 19 SHOWING ELLIPSOID HEIGHT VARIATION

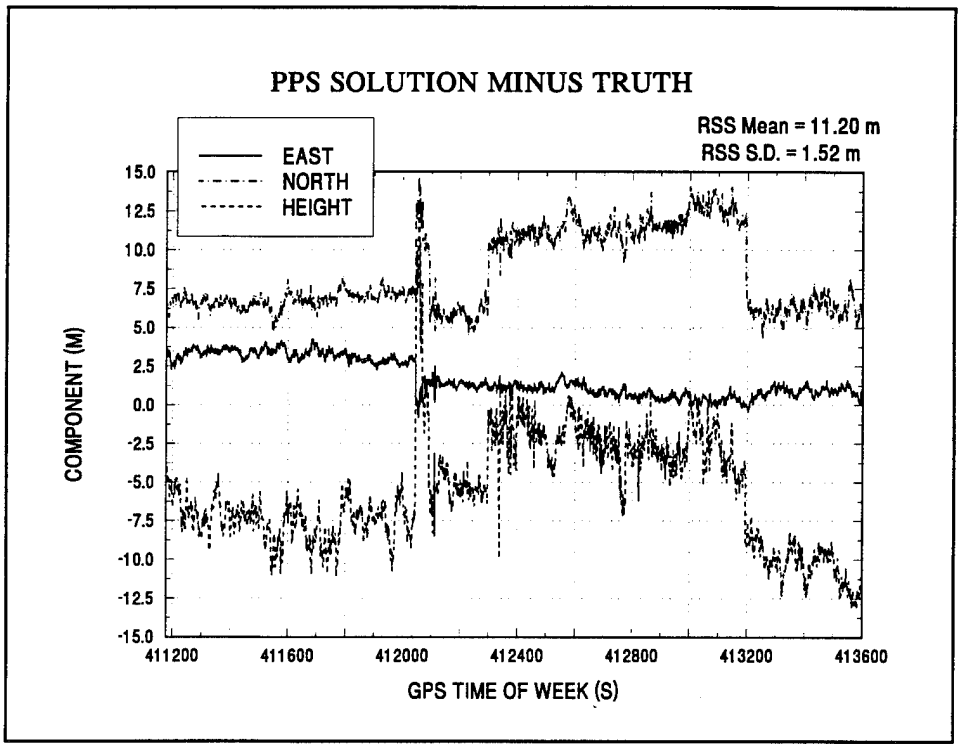

FIGURE 31. DIFFERENCE BETWEEN PPS SOLUTIONS AND TRUTH FOR VEHICLE CIRCUIT AT DAHLGREN

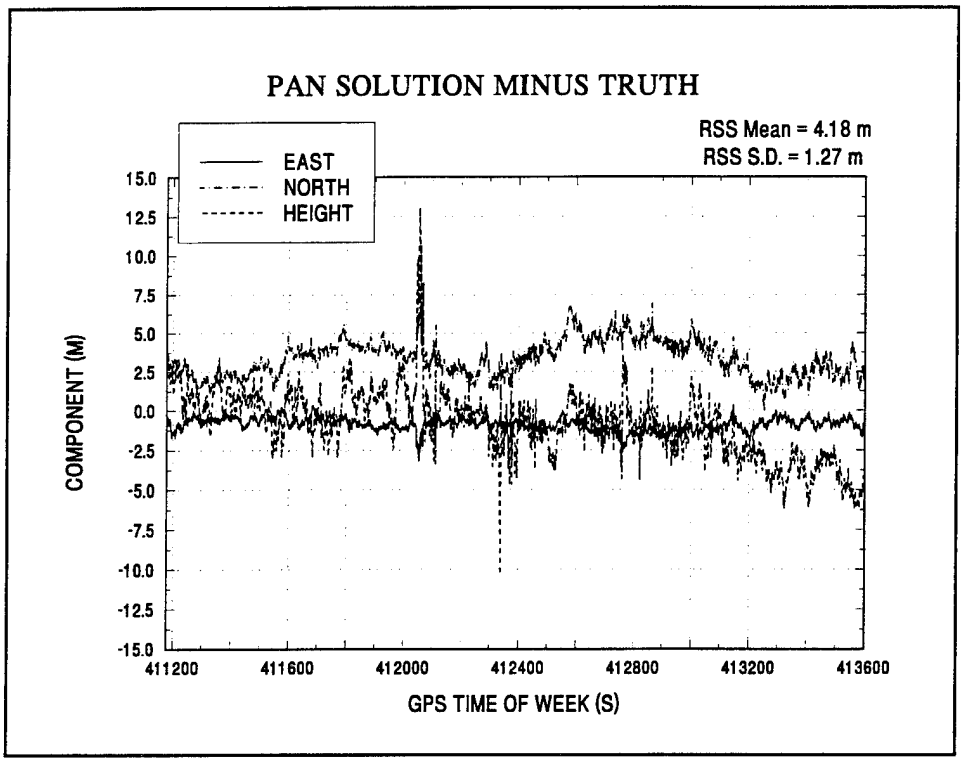

FIGURE 32. DIFFERENCE BETWEEN PAN SOLUTION AND TRUTH FOR VEHICLE CIRCUIT AT DAHLGREN

TABLE 5. DIFFERENCE TABLE FOR VEHICLE SOLUTIONS AROUND DAHLGREN CIRCUIT

UNIT: METERS	PPS SOLUTIONS				PAN SOLUTIONS			
	EAST	NORTH	HEIGHT	RANGE	EAST	NORTH	HEIGHT	RANGE
MEAN	1.73	8.49	-5.67	11.20	-0.90	3.36	-0.82	4.18
SD	1.21	2.59	3.54	1.52	0.43	1.17	2.17	1.27

METHOD

The satellite range corrections can be found from data collected at static sites whose position is already well known. There were two such sites during the dynamic vehicle tests, the site at Dahlgren (MBRE), and the site at Corbin, Virginia, 33 km southwest (ASTW). Since the navigation solutions are independent from one time to the next, the range corrections need to be obtained in a similar manner. If there are n satellites in common view at site k, then there are n pseudorange observations. The unknowns include the local clock bias and the n satellite range biases. It will be assumed that the site coordinates are known. If the unknown local clock bias is lumped in with the satellite range biases, then it can be removed from the problem by differencing.

One satellite was selected as the reference and arbitrarily assigned zero range bias. The computed ranges were constructed from the satellite ephemerides, clock predictions, and the known site position. The reference satellite range was subtracted from all the others leaving $n-1$ observations and $n-1$ unknowns that, in principle, could be solved. Since there were actually two static sites, there were $2(n-1)$ observations and $n-1$ unknowns. The problem was over-determined and least squares estimation could be used.

These range biases were then treated as range corrections and subtracted from the computed ranges at each dynamic site. The fact that one satellite was given a zero bias, when in fact it was not zero, does not matter when the corrections are made, as long as the determination of the *true* vehicle clock offset is not important. The range corrections just add the reference satellite range bias to the local clock offset, and the combined offset is solved in the usual way during the navigation solution. These postprocessed navigation solutions are differential solutions because they depend upon information supplied by static sites whose positions are known. All common range biases, such as dither, radial orbit error, residual satellite clock estimation error, and correlated refractions errors, are therefore removed and the navigation solutions are improved.

RESULTS

Examples of the range corrections are shown in Figure 33 with PRN14 as the reference satellite. The degree to which the curves are correlated is the result of the common time-varying range bias from the reference satellite and the local clock.

Figures 34 and 35 show the results obtained from the differentially corrected observations. These should be compared to Figures 25 and 26, which show the original uncorrected SPS solutions. Since the purpose was to eliminate only the dither component of SA, these differential solutions could not be used as the equivalent to the PPS solutions. The PPS solutions include the orbit error from the broadcast ephemerides, whereas the differentially corrected solutions have some of the orbit error (and other effects) removed. Table 6 summarizes the differences between the differentially corrected solutions and truth. Notice that the mean errors are smaller than either the PPS or the PAN solutions listed in Table 5. The standard deviations are similar to the PAN solutions.

The differences between the SPS and the differentially corrected SPS solutions vs. time are illustrated in Figures 36 and 37. Notice that the scale for the component axis is ±100 m in the case of the SPS results, and ±15 m in the differentially corrected case. Since the differentially corrected solutions were not representative of the PPS results, they were not used for evaluation of the PAN solutions. Instead, the data files and broadcast ephemerides for all four sites were corrected by DMA in their DCF.

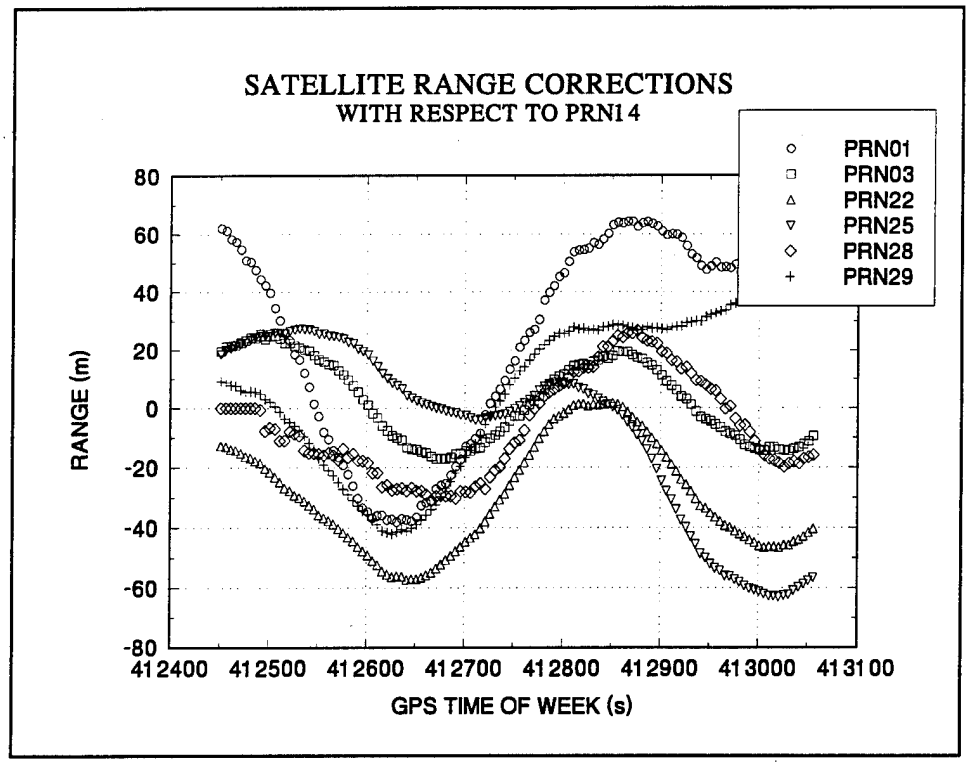

FIGURE 33. SATELLITE RANGE CORRECTIONS DURING DYNAMIC VEHICLE CIRCUIT AT DAHLGREN

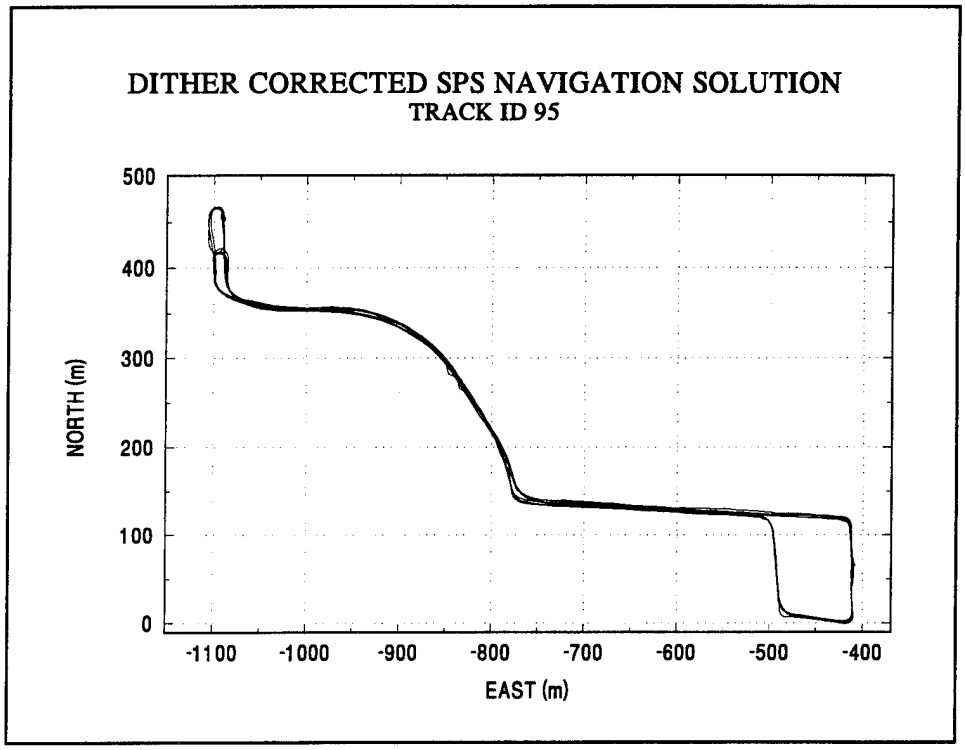

FIGURE 34. DIFFERENTIALLY CORRECTED SPS SOLUTIONS USING RANGE CORRECTIONS

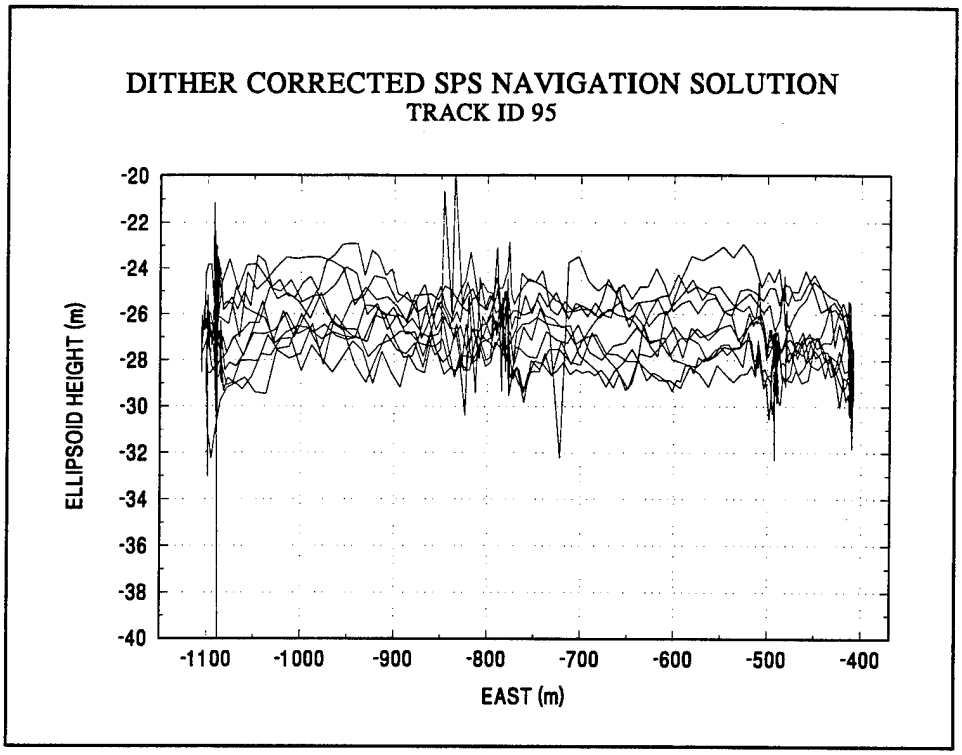

FIGURE 35. DIFFERENTIALLY CORRECTED SPS SOLUTIONS USING RANGE CORRECTIONS

TABLE 6. DIFFERENCES BETWEEN SPS OR DIFFERENTIALLY CORRECTED SPS SOLUTIONS AND TRUTH

UNITS: METERS	SPS SOLUTIONS				CORRECTED SPS SOLUTIONS			
	EAST	NORTH	HEIGHT	RANGE	EAST	NORTH	HEIGHT	RANGE
MEAN	-5.20	18.72	-20.85	56.84	0.07	-0.07	0.35	1.82
SD	19.65	21.79	50.00	30.68	0.62	1.10	1.64	1.06

DISCUSSION

This investigation has demonstrated that PPS navigation solutions from field sites can be upgraded to precise-ephemerides quality without reprocessing the original observations. If files are kept of the unclassified navigation solutions, the time, and the satellites being tracked, and a source of the SA-corrected broadcast ephemerides and precise ephemerides are available, then the PPS solutions obtained with the broadcast ephemerides can be improved at a later date. This PAN capability can make important contributions to military mapping operations where vehicles equipped with PPS receivers can gain access to areas lacking geodetic control points.

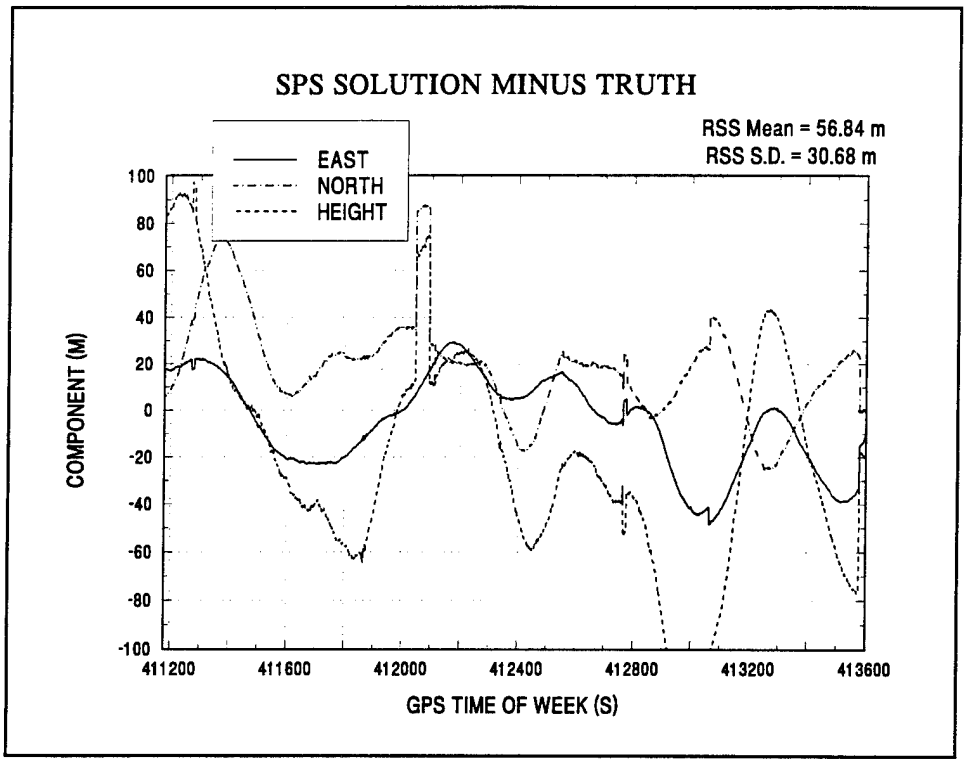

FIGURE 36. DIFFERENCE BETWEEN SPS SOLUTIONS AND TRUTH FOR DYNAMIC VEHICLE 95

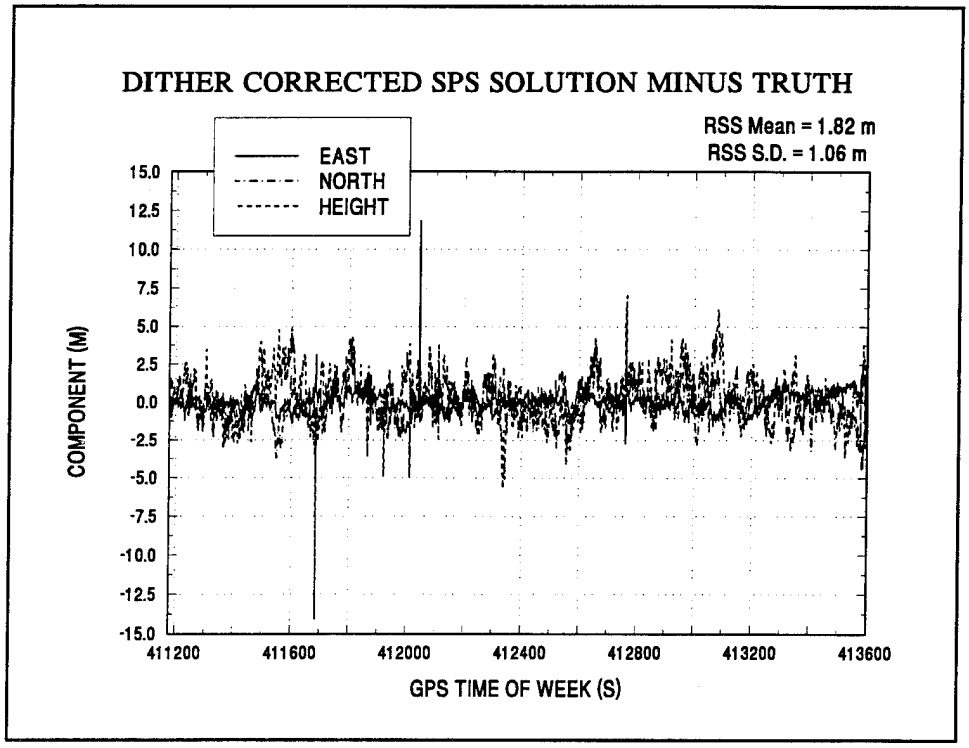

FIGURE 37. DIFFERENCE BETWEEN CORRECTED SPS SOLUTIONS AND TRUTH FOR DYNAMIC VEHICLE 95

PAN PROGRAM DESCRIPTION

In developing the code for PAN, programming methodologies of portability, readability, and error analysis were taken into consideration. ANSI standards and machine-independent code were used to allow the program to be executed on more than one platform. Prologues at the beginning of each subroutine, comments throughout the subroutines, as well as descriptive names for variables and routine names were some measures taken to make the code more readable. The program was compiled and tested in small components, debug print statements were placed throughout the program, and intermediate results were compared for accuracy to enhance the error analysis process. The code was also processed through a FORTRAN code checker that had the capabilities to find programming errors the compiler might have missed, such as undefined variables and call-line inaccuracies.

The top-down design approach of starting with a problem and breaking the problem into smaller tasks was used in developing this code. First, an outline was developed from the formulation. This outline then was used as a basis for developing pseudo-code. Modular routines, where each different task is developed into its own subroutine, were developed using the pseudo-code as a basis. Routines for some of the tasks involving matrix computation and interpolation already existed in mathematical utility libraries. These existing routines were merged into a library directory that would later be linked with the program. Include files were also used for all global variables.

PAN has the capabilities to solve for one of the following options over a user-specified time interval:

- Solve for a PPS solution using broadcast ephemerides,
- Solve for a PE solution using precise ephemerides,
- Solve for both PPS and PE solutions.

The input requirements for PAN are:

- A configuration file
- 1 RINEX Navigation file
- 1 RINEX Observation file

If the user is solving for PE solution, then the following files are also needed:

- 1 to *n* Satellite Trajectory files in PC ASCII format
- 1 Satellite Clock file in PC ASCII format

If the user is solving for just PE, then the user needs to input:

- A PPS solution file

The configuration file is a file containing all user input parameters needed for execution. This file uses keyword specification in that it searches for keywords in the file to indicate what the parameter values are. This allows the user to put the parameters in any order in the file, as well as to freely put comments throughout the configuration file. The keyword search method also allows the user to omit unnecessary parameters from the configuration file. With the keyword specification method, the program can be easily modified to add new input parameters. This method also gives the user more flexibility in modifying the configuration file. A full description of the different input parameters that are acceptable by PAN can be found in the PAN User's Guide section.

The user can execute the program from the DOS prompt with the following command:

>pan.exe or fullpath if not in directory containing exe

After the user types in the above command, the following line will appear on the screen, and the user can then type in the configuration filename as indicated by italics:

Enter configuration filename (40 chars max):
c:\pan\datapc\view.cfg

The program will then begin processing solutions for each time step in the given interval. If the user wishes to have debug statements printed out, this option is available. The output files consist of either one or two files, depending on whether the option to compute the PPS solution, the PE solution, or both, was chosen. The output files will contain the X, Y, Z solutions (meters), the clock solution (meters), the solution in longitude and latitude (degrees), the east, north, and vertical differences, the RSS of residuals, and the GDOP solution. A description of these output files can be found in the PAN User's Guide section.

PAN was written in FORTRAN and complied and executed on several different platforms including several different PC models, and an RISC 6000. PAN contains approximately 6600 lines of code separated into three different directories:

- DITHER 5 routines
- PAN 25 routines
- LIB 34 routines

PAN took 55 sec to complete the execution of a case that was set up to solve for both the PE and PPS solution for six satellites over a 20-sec time interval with a step size of 1 sec. In a similar case, solving for both solutions using 25 satellites over a 120-sec time interval using a time step of 30 sec, the program took 3 min to complete.

PAN USER'S GUIDE

This program has the ability to improve PPS Absolute Navigation Solutions so that they approach the quality that is achievable from the DMA precise ephemerides and clock. Real-time navigation solutions necessarily need to use the broadcast ephemerides as the source of the satellite's position and clock, and therefore include the satellite prediction errors in the solution. Since the precise ephemerides and clock is a smoothed fit that is not available in real time, it avoids the prediction errors and consequently allows significantly better results to be realized.

PROGRAM STRUCTURE

PAN involves two major tasks. First the program solves the PPS equivalent solution by the following steps:

1. Reads in RINEX observation files and satellite ephemeris files.
2. Implements the satellite ephemeris algorithm.
3. Chooses the correct ephemeris message and evaluates the satellite position at the time of transmission for each observation.
4. Finds the ionospherically corrected pseudorange from the "raw" pseudoranges.
5. Forms the O_o vector from the pseudorange.
6. Forms the C_o vector from the broadcast ephemeris and an estimate of the current absolute position.
7. Computes the partial derivatives.
8. Solves for a navigation solution at each time step.

Second, the program converts the PPS solution to the precise-ephemerides equivalent by the following method:

1. With the PPS navigation solution at each time step and the broadcast ephemerides, it forms the computed range vector C_b.
2. With the PPS navigation solution at each time step and the precise ephemerides, it forms the computed range vector C_p.
3. Computes the partial derivatives from the PPS solution and the precise ephemerides.
4. Solves for the PAN solution.

PAN is set up so the user can either solve for the PPS solution, the PPS solution and PE solution, or just the PE solution. The program uses the set of satellite PRN numbers on the observation file to solve the PPS solution. For the PE solution, the user needs to list the satellite PRN numbers to solve for in the configuration file. There must be a trajectory file for each satellite specified, and these satellite PRN numbers must appear on the satellite clock file, as well as on the Broadcast Ephemeris file. If the user selects to just solve for the PE solution, an input file containing PPS solution for the time ranch must be available. If a satellite contains events in the satellite clock file, this satellite will be omitted from solving the PE solution.

PROGRAM EXECUTION

PAN will ask for a configuration filename. Enter the name and pathname (up to 40 characters). PAN will execute over an interval of time and output several files depending on the user options.

FILE INPUT/OUTPUT

Pan Input

A configuration file
1 RINEX Navigation File
1 RINEX Observation File
1 - MAXSAT Satellite Trajectory Files (PC ASCII formatted)
(only needed if solving for PE solution)
1 Satellite Clock File (PC ASCII formatted) (only needed for PE)
DITHER output file containing dither estimations (optional file not needed for PAN)
PSS Solution File (only needed if solving for PE only)

Pan Output

One to four output files can be generated giving solutions in different formats. Either a file with PPS solution results or a file with PE solution results.

FILE FORMATS

Pan Configuration File

There is no specific order to the placement of input values in the file. The program searches for keywords within the configuration file. These keywords must be placed at the start of a line. Comment lines are represented by "#" signs and ignored by the program.
Here is a list of valid keywords:

NAV	RINEX Navigation file name (max 40 char)
OBSERV	RINEX Observation file name (max 40 char)
T	Trajectory Filenames (max 40 char)
C	Satellite Clock filename (max 40 char)

The configuration file can have either one or both of the following output files.

OTPPS	create output file for PPS solution (filename)
OTPE	create output file for PE solution (filename)

WEEK	GPS week #
TIME	Start time End time (seconds into GPS week)
RUNTYPE	Indicates what type of run to execute (1=PPS only; 2=PPS and PE; 3=PE only)

LL has four variables on the line: IOPT (which tells program if the latitude and longitude position are in degrees or radians), latitude position, longitude position, and height.

LL	IOPT (0=degrees 1=radian) LAT LONG HEIGHT

The following are optional (These can be put in the configuration file if the user wants to change the default values):

INTERVAL	time step (default value = 1)
TEMP	temperature (default value = 280 KELVIN)
PRESSURE	pressure (default value = 990 millibar)
HUM	humidity (default value = 50%)
D	Dither Estimation File (40 chars max)
PELIST	List of satellite PRN#s to solve PE solution for (default list: 1 2 3 4 5)
PPSFILE	Input PPS filename (40 chars max) (must have if RUNTYPE = 3)
DEBUG	1 (option to turn on debug statements) (default = 0 ---- do not print out)

A sample PAN configuration is shown Figure 38.

PPS Solution Input File Format

Each line contains: time xsoln ysoln zsoln clockoffset.
format: 1x,i7,4d17.10

Pan Output File (for both PPS and PE solution files)

One record for each time processed with the following format:

time of week (sec)	---- f8.0
x solution (m)	---- f13.3
y solution (m)	---- f13.3
z solution (m)	---- f13.3
clock solution (sec)	---- f13.10
longitude (degrees)	---- f13.8 (ex. 282.12345678)

latitude (degrees)	---- f13.8
ellipsoid height (m)	---- f12.4
longitude (integer part only)	---- i5 (ex. 282)
latitude (integer part only)	---- i5
longitude (decimal part only)	---- f12.8 (ex. .12345678)
latitude (decimal part only)	----f12.8
east difference (m)	---- f12.4
north difference (m)	---- f12.4
vertical difference (m)	---- f12.4
RSS of residuals (m)	---- f12.4
GDOP	---- f10.2

```
#This is a sample configuration file using default values
# solve for both PPS and PE solutions
RUNTYPE 2
# list of satellites to solve PE solution for
PELIST 1 14 22 25 27 29 31
NAV c:\pan\data\4872048b.nav
OBSERV c:\pan\data\4872048b.rnx
T c:\traj\P001736
T c:\traj\P002736
T c:\traj\P014736
T c:\traj\P022736
T c:\traj\P025736
T c:\traj\P029736
T c:\traj\P031736
C c:\traj\GC736
# This case is to include dither file
D c:\dither\dithot
# Want both output files
OTPPS out1.pps
OTPE  out1.pe
WEEK 736
# time interval (start and end time (secs)
TIME 411062 411065
# lat long in radian
LL 1 0.669d0 4.938604d0 -29.00009d0
#End of sample configuration file
#####################################################
```

FIGURE 38. PAN CONFIGURATION FILE

PRODUCT DISCLAIMER

The mention of a commercial company or product does not constitute an endorsement by NSWCDD or DMA. The information in this paper is not authorized for use for publicity or advertisements.

REFERENCES

1. Hermann, Bruce R., "Five Years of Absolute Position at the Naval Surface Warfare Center," *Proceedings of the Sixth International Geodetic Symposia on Satellite Positioning*, The Ohio State University, Mar 1992.

2. Malys, Stephen; Bredthauer, Dennis; Hermann, Bruce; and Clynch, James, "Geodetic Point Positioning with GPS: A Comparative Evaluation of Methods and Results," *Proceedings of the Sixth International Geodetic Symposium on Satellite Positioning*, The Ohio State University, Mar 1992.

3. Lachapelle, G.; Klukas, R.; Roberts, D.; Qui, W.; and McMillian, C., "One-Meter Level Kinematic Point Positioning Using Precise Orbits and Satellite Clock Corrections," *Proceedings on ION GPS-94*, Salt Lake City, UT, Sep 1994.

4. Leach, Mark, private communication: Applied Research Laboratory at the University of Texas at Austin, 15 Sep 1995.

5. Hermann, B. R.; Evans, A.; Law, C.; and Remondi, B., "Kinematic On-The-Fly GPS Positioning Relative to a Moving Reference," *Proceedings of ION GPS-94*, Salt Lake City, UT, Sep 1994.

6. Malys, S. and Ortiz, M., "Geodetic Absolute Positioning with Differenced GPS Carrier Beat Phase Data," *Proceedings of the 5th International Geodetic Symposium on Satellite Positioning*, Las Cruces, NM, Mar 1989.

APPENDIX A

PRECISE ABSOLUTE NAVIGATION (PAN) FORMULATION

VERSION: 1.4

PRECISE ABSOLUTE NAVIGATION FORMULATION

Bruce R. Hermann K12
Naval Surface Warfare Center, Dahlgren Division
Updated: 22 September 1995

DESCRIPTION

This task will develop a capability to improve Precise Positioning Service (PPS) absolute navigation solutions so that they approach the quality that is achievable from the Defense Mapping Agency (DMA) precise ephemerides and clock. Real-time navigation solutions necessarily use the broadcast ephemerides as the source of the satellite's position and clock and, therefore include satellite prediction errors in the solution. Since the precise ephemerides-and-clock is a smoothed fit that is not available in real time, it avoids prediction errors and consequently allows significantly better results to be realized.

ASSUMPTIONS

The Global Positioning System (GPS) time and the PPS solutions to be improved are given, as is the receiver type and the version of the navigation algorithm used. Algorithm information will be used to establish which satellites, of those in view, produced the particular navigation solution. To compute the difference between the ephemerides, an independent source of the Selective Availability-(SA-)corrected broadcast ephemerides and the DMA precise-ephemerides-and-clock are required. Finally, for testing purposes, raw pseudorange and phase observations from a typical receiver will be needed in addition to the information above.

METHOD

Satellite ephemerides, clocks, and the PPS solution are given. The form of the observation equations that produced the navigation solution can be reconstructed as in Equation (A-1). The original vector of observation was O_0, the computed ranges were in the C_0 vector, and the initial state vector was X_0. None of these vectors were saved.

$$O_0 = C_0 + \frac{\partial C_0}{\partial X_0} \Delta X_0 \qquad \text{(A-1)}$$

The solution toEquation (A-1) is ΔX_0, from which the new state vector X_b (the PPS solution) is found: $X_b = X_0 + \Delta X_0$. Since the same observations would be used regardless of the ephemerides, the observation equations using the broadcast ephemerides (subscript b) can be equated to the equations using the precise ephemerides (subscript p) inEquation (A-2).

$$C_b + \frac{\partial C_b}{\partial X_b} \Delta X_b = C_p + \frac{\partial C_p}{\partial X_p} \Delta X_p \qquad \text{(A-2)}$$

The given PPS navigation solution X_b is used in the computation for the vector C on both sides of Equation (A-2). Assuming operation in the linear region, the solution from Equation (A-1) used

along with the original satellite ephemerides to compute C_b should require no further correction. This makes $\Delta X_b \approx 0$. Therefore Equation (A-2) can be rearranged into a form similar to that in Equation (A-1). The result, Equation (A-3), can be solved in the usual least squares sense to obtain the correction ΔX_p that should be applied to the given X_b to form the precise solution: $X_p = X_b + \Delta X_p$.

$$C_b - C_p = \frac{\partial C_p}{\partial X_p} \Delta X_p \qquad \text{(A-3)}$$

TASK OUTLINE

PPS EQUIVALENT SOLUTION

1. Read RINEX observation files and satellite ephemeris files.
2. Implement the satellite ephemeris algorithm.
3. Choose the correct ephemeris message, and evaluate the satellite position at the time of transmission for each observation.
4. Check the phase observations for cycle jumps.
5. Smooth the pseudoranges with the phase observations.
6. Form the O_0 vector from the smoothed pseudoranges for use in Equation (A-1).
7. Form the C_0 vector from the broadcast ephemeris and an estimate of the current absolute position.
8. Compute the partial derivatives for use in Equation (A-1).
9. Solve for a navigation solution at each time step and save the results.

CONVERT PPS SOLUTION TO THE PRECISE EPHEMERIDES EQUIVALENT:

1. With the PPS navigation solution at each time step and the broadcast ephemerides, form the computed range vector, C_b in Equation (A-3).
2. With the PPS navigation solution at each time step and the precise ephemerides, form the computed range vector, C_p in Equation (A-3).
3. Compute the partial derivatives from the PPS solution and the precise ephemerides.
4. Solve Equation (A-3) for the precise absolute navigation solution.
5. Compare the PPS solutions with the truth.

The code should be developed in FORTRAN or C so that it can be compiled on a single-user PC as well as a workstation. The data files for the equivalent PPS solution are currently in RINEX format on PC-compatible disks. The precise ephemerides are available from OMNIS files for GPS week 736.

CONFIGURATION INPUT FILE

The user will interface with the program through a configuration file. This ASCII file will contain the information needed by the program to perform the computations. The user can keep copies of several files with different names for different data spans. The file will include the following information:

1. RINEX data file name
2. RINEX navigation file name.
3. Precise ephemeris file names, one per satellite.

4. Precise clock file name.
5. Initial site position: longitude, latitude, height (deg, deg, m).
6. Start and stop times (GPS time of week in seconds).
7. A list of satellite PRN numbers to omit from processing.

GENERATE AN EQUIVALENT PPS NAVIGATION SOLUTION

In the operational environment, the PPS navigation solutions will be obtained from the field. Presumably these solutions were obtained with a receiver that can correct for the effects of Selective Availability (SA) and AntiSpoofing (AS). AS encrypts and SA corrupts the GPS signals making the precise signal and the full accuracy of the broadcast ephemerides accessible to authorized users only. These receivers can display the navigation solution in real time, but the field-corrected satellite ephemerides and observations are classified and therefore are not available to the user. For this demonstration, the equivalent to a PPS solution needs to be computed from known observations, with a known algorithm, and with known satellite ephemerides.

The equivalent PPS solution used to demonstrate the method is derived from data that do not have the effects of SA (epsilon) removed from the broadcast ephemerides or SA (dither) from the satellite frequency standard, but does provide dual frequency pseudorange. These data were obtained with Trimble 4000SSE receivers as part of the Evans Drive-By experiment performed in February 1994.[A-1] The Trimble 4000SSE receiver gives L_1 C/A and the cross correlation between L_1 and L_2 Y codes (when AS is implemented) to provide the L_2 pseudorange observation. The dual frequency phase observations are also available.

GPS OBSERVATION MODEL

For best results, on-the-fly (OTF) relative positioning requires the use of both pseudorange and phase observations at L_1 and L_2 frequencies. An observation model that describes the pseudorange was presented by Braasch.[A-2] See Figure A-1. The notation will be modified for the purposes here, but the general form will be retained. For each parameter, a dependance upon satellite will be expressed as a superscript j or k; a dependance upon receiver will be expressed by a subscript m or n. The transmission frequency is denoted by the subscript f, which may be either a 1 or 2, and the time of the observation by the subscript i. Absence of a dependance is represented by a dot.

Braasch's observation equation includes the following terms: the true geometric range $r^j_{m.i}$ between receiver antenna m and the satellite j at epoch t_i; the receiver time offset $\tau_{m.i}$; the satellite time offset $\tau^j_{..i}$; propagation effects due to the troposphere $T^j_{m.i}$ and the ionosphere $I^j_{mfi} = (\lambda^2_f/c)\, K^j_{m.i}$; the User Range Error URE; multipath error d_{MP}; receiver satellite channel delay d_{HW}; receiver measurement bias errors d_{MEAS}; receiver noise; and the deliberately introduced effects of Selective Availability $SA^j_{..i}$. In the following development, the User Range Error, multipath error, receiver channel delay, bias errors, and noise will be omitted, but a term is added to account for relativistic effects $\gamma^j_{m.i}$. The ionospheric constant $K^j_{m.i}$ is related to the columnar electron content. The pseudorange observation ρ^j_{mli} for satellite j, receiver m, frequency l, and observation i, with meters as units, is written in Equation (A-4).

$$\rho^j_{mli} = r^j_{m.i} + \gamma^j_{m.i} + c\,(\tau_{m.i} - \tau^j_{..i}) + T^j_{m.i} + \frac{\lambda^2_l}{c} K^j_{m.i} + SA^{\,j}_{\,.i} \qquad \text{(A-4)}$$

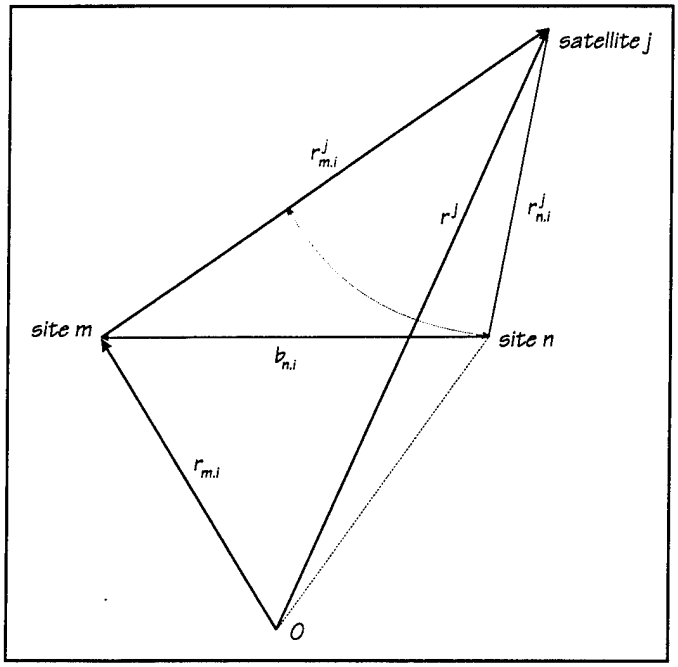

FIGURE A-1. ONE-SATELLITE, TWO-SITE GEOMETRY

A similar expression can be used for the phase observation if an integer cycle ambiguity term N^j_{m10} is added. It represents the number of full cycle counts recorded by the receiver on a particular channel and is arbitrary. Since the integer cycle term is part of the observation, it will be included on the left-hand side in Equation (A-5). The phase Φ^j_{m1i} (cycles) represents the observed range $R^j_{m.i}$ (meters) divided by the wavelength (meters), so the result has units of cycles. Both N^j_{m10} and Φ^j_{m1i} have units of cycles, so the wavelength λ_1 is needed to change these cycles back to meters. Note that the ionospheric refraction in Equation (A-5) has the opposite sign than it had in Equation (A-4).[A-3]

$$\lambda_1 (\Phi^j_{m1i} + N^j_{m10}) = r^j_{m.i} + \gamma^j_{m.i} + c(\tau_{m.i} - \tau^j_{..i}) + T^j_{m.i} - \frac{\lambda_1^2}{c} K^j_{m.i} + SA^j_{..i} \qquad \text{(A-5)}$$

The geometric range $r^j_{m.i}$ is the magnitude of the vector to the satellite, in the WGS84 coordinate system, minus the vector to the receiver antenna, as shown in Equation (A-6). The satellite coordinates as a function of time are available from the satellite ephemerides, while the receiver antenna coordinates are to be found.

$$\mathbf{r}^j_{m.i} = \mathbf{r}^j_{..i} - \mathbf{r}_{m.i} = (x^j_{..i} - x_{m.i})\hat{x} + (y^j_{..i} - y_{m.i})\hat{y} + (z^j_{..i} - z_{m.i})\hat{z} \qquad \text{(A-6)}$$

SMOOTHING PSEUDORANGE WITH PHASE (Not Implemented)

As shown in Equation (A-5), the phase observations have an unknown tracker bias N^j_{m10} that is site-, satellite-, and frequency-dependent. Therefore, the phase observations cannot be used to obtain a navigation solution in the same manner as the pseudoranges, because there is an added unknown

range bias introduced by each satellite. This is unfortunate, because the noise associated with a single-frequency pseudorange observation is about an order-of-magnitude greater than the noise on the equivalent phase observation. Multipath is also less pronounced with phase. For these reasons, when pseudoranges are needed but an instantaneous real-time navigation solution is not the primary objective, it is advantageous to use the phases to smooth the pseudoranges.

SINGLE FREQUENCY OBSERVATIONS

In order to smooth the pseudoranges, continuous uninterrupted phase observations from all satellites are required over the entire period of interest. The idea is to reduce the error on the initial pseudorange observation by averaging. In effect, the pseudoranges at any time t_i become the sum of the initial averaged pseudorange, plus the difference between the phase observation at t_i and the initial phase at t_0. In practice, phase observations will be interrupted from time to time for a variety of reasons; consequently, it is prudent to plan for these interruptions. To do this, data from each satellite must be processed independently, because the phase interruptions can occur at different times on different satellites. Over the time period of interest, several interruptions can be expected to occur on a given satellite; so the pseudorange averaging must be recomputed after each continuous span. The smoothing process is demonstrated in the equations that follow.

By differencing between Equations (A-4) and (A-5), all the terms on the right-hand side are removed except for the ionospheric component. This result for t_i is shown in Equation (A-7).

$$\rho^{j}_{m1i} - \lambda_1 (\phi^{j}_{m1i} + N^{j}_{m10}) = 2 \frac{\lambda_1^2}{c} K^{j}_{m.i} \qquad \text{(A-7)}$$

By differencing in time two equations like Equation (A-7), the unknown integer N^{j}_{m10} can be removed. Equation (A-8) shows the difference between observations at t_i and t_0.

$$\rho^{j}_{m1i} - \rho^{j}_{m10} = \lambda_1 (\phi^{j}_{m1i} - \phi^{j}_{m10}) + 2 \frac{\lambda_1^2}{c} (K^{j}_{m.i} - K^{j}_{m.0}) \qquad \text{(A-8)}$$

Equation (A-8) can be rearranged so that all the terms relating to t_0 are on the left-hand side. They are expressed in terms of the pseudorange and ionospheric term at each succeeding time, plus the phase differences as shown in Equation (A-9).

$$\rho^{j}_{m10} - 2 \frac{\lambda_1^2}{c} K^{j}_{m.0} = \rho^{j}_{m1i} - 2 \frac{\lambda_1^2}{c} K^{j}_{m.i} - \lambda_1 (\phi^{j}_{m1i} - \phi^{j}_{m10}) \qquad \text{(A-9)}$$

The average pseudorange, denoted by the overbar in Equation (A-10), is evaluated at t_0 by summing Equation (A-9) over all κ observation times.

$$\overline{\rho^{j}_{m10} - 2\frac{\lambda_1^2}{c}K^{j}_{m.0}} = \frac{1}{\kappa + 1}\sum_{i=0}^{\kappa}\left[\rho^{j}_{m1i} - 2\frac{\lambda_1^2}{c}K^{j}_{m.i} - \lambda_1(\phi^{j}_{m1i} - \phi^{j}_{m10})\right] \tag{A-10}$$

Now the pseudorange at each time, t_i, can be reconstructed by rearranging Equation (A-9) and inserting the average value for the pseudorange at t_0 from Equation (A-10). The result, Equation (A-11), is the smoothed pseudorange observation equation for L_1. If L_2 observations are available, the same procedure can be applied to them. In cases where two-frequency data are available, it may be useful to remove the ionospheric term. This procedure is discussed in the next section.

$$\rho^{j}_{m1i} - 2\frac{\lambda_1^2}{c}K^{j}_{m.i} = \overline{\rho^{j}_{m10} - 2\frac{\lambda_1^2}{c}K^{j}_{m.0}} + \lambda_1(\phi^{j}_{m1i} - \phi^{j}_{m10}) \tag{A-11}$$

DUAL FREQUENCY OBSERVATIONS

When dual-frequency observations are available, the ionospheric term may be removed before computing the smoothed pseudorange. The pseudorange time difference, derived from Equation (A-4), is shown in Equation (A-12); and the phase time difference, derived from Equation (A-5), is shown in Equation (A-13). Assuming that there are no phase jumps between epochs t_0 and t_i, the integer cycle term N^{j}_{m1}. subtracts out in Equation (A-13).

$$\begin{aligned}\rho^{j}_{m1i} - \rho^{j}_{m10} = {} & \frac{\lambda_1^2}{c}(K^{j}_{m.i} - K^{j}_{m.0}) + \\ (r^{j}_{mi.} - r^{j}_{m.0}) + (\gamma^{j}_{m.i} - \gamma^{j}_{m.0}) + c(\tau_{m.i} - \tau_{m.0}) - c(\tau^{j}_{..i} - \tau^{j}_{..0}) + & \\ (T^{j}_{m.i} - T^{j}_{m.0}) + (SA^{\,j}_{..i} - SA^{\,j}_{..0}) & \end{aligned} \tag{A-12}$$

$$\begin{aligned}\lambda_1(\phi^{j}_{m1i} - \phi^{j}_{m10}) = {} & -\frac{\lambda_1^2}{c}(K^{j}_{m.i} - K^{j}_{m.0}) + \\ (r^{j}_{m.i} - r^{j}_{m.0}) + (\gamma^{j}_{m.i} - \gamma^{j}_{m.0}) + c(\tau_{m.i} - \tau_{m.0}) - c(\tau^{j}_{..i} - \tau^{j}_{..0}) + & \\ (T^{j}_{m.i} - T^{j}_{m.0}) + (SA^{\,j}_{..i} - SA^{\,j}_{..0}) & \end{aligned} \tag{A-13}$$

The ionospheric term can be computed from Equation (A-13) if two-frequency phase data are available. First, form the differences as in Equation (A-13) for both L_1 and L_2. Then difference the two time differences. All the terms on the right in Equation (A-13) are independent of frequency except the ionospheric term. The result of the difference is written as Equation (A-14).

$$\lambda_1(\Phi^j_{m1i} - \Phi^j_{m10}) - \lambda_2(\Phi^j_{m2i} - \Phi^j_{m20}) = \left(\frac{\lambda_2^2 - \lambda_1^2}{c}\right)(K^j_{m.i} - K^j_{m.0}) \quad \text{(A-14)}$$

Each of the ionospheric terms is modeled by a frequency-independent parameter $K^j_{m.i}$, which represents the electron content along the line of sight, between each receiver antenna and each satellite. A solution for the constants is possible in terms of the phase observations and their respective wavelengths as shown in Equation (A-15).

$$K^j_{m.i} - K^j_{m.0} = c\left(\frac{\lambda_1(\Phi^j_{m1i} - \Phi^j_{m10}) - \lambda_2(\Phi^j_{m2i} - \Phi^j_{m20})}{\lambda_2^2 - \lambda_1^2}\right) \quad \text{(A-15)}$$

If Equation (A-15) is multiplied by $2(\lambda^2_1/c)$ and added to both sides of Equation (A-13), a time-differenced observation is created that has the same right-hand side as the pseudorange time difference Equation (A-12). Equation (A-16) shows that this form has the same functional properties as the pseudorange, but with the low noise properties of phase.[A-3]

$$\begin{aligned}\lambda_1(\Phi^j_{m1i} - \Phi^j_{m10}) + 2\lambda_1^2\left(\frac{\lambda_1(\Phi^j_{m1i} - \Phi^j_{m10}) - \lambda_2(\Phi^j_{m2i} - \Phi^j_{m20})}{\lambda_2^2 - \lambda_1^2}\right) = \\ \frac{\lambda_1^2}{c}(K^j_{m.i} - K^j_{m.0}) + (r^j_{m.i} - r^j_{m.0}) + (\gamma^j_{m.i} - \gamma^j_{m.0}) + \\ c(\tau_{m.i} - \tau_{m.0}) - c(\tau^j_{..i} - \tau^j_{..0}) + (T^j_{m.i} - T^j_{m.0}) + (SA^{\,j}_{..i} - SA^{\,j}_{..0})\end{aligned} \quad \text{(A-16)}$$

Since the right-hand side of Equation (A-16) is the same as the right-hand side of Equation (A-12), the left-hand sides of those two equations must be equal. Exploiting this, the pseudorange at t_i can be rewritten in terms of the two-frequency phase observations and the pseudorange at t_0 as in Equation (A-17). A similar expression can be written for L_2.

$$\rho^j_{m1i} = \rho^j_{m10} + \lambda_1(\Phi^j_{m1i} - \Phi^j_{m10}) + 2\lambda_1^2\left(\frac{\lambda_1(\Phi^j_{m1i} - \Phi^j_{m10}) - \lambda_2(\Phi^j_{m2i} - \Phi^j_{m20})}{\lambda_2^2 - \lambda_1^2}\right) \quad \text{(A-17)}$$

Equation (A-17) can be rearranged to find an average value for ρ^j_{m10}, as was done for the single frequency case. This average can then be substituted into Equation (A-17) and the smoothed pseudoranges computed from the phases. Equation (A-18) is used to compute this average pseudorange at t_0.

$$\overline{\rho^j_{m10}} = \frac{1}{\kappa + 1}\sum_{i=0}^{\kappa}\left\{\rho^j_{m1i} - \lambda_1(\Phi^j_{m1i} - \Phi^j_{m10}) - 2\lambda_1^2\left(\frac{\lambda_1(\Phi^j_{m1i} - \Phi^j_{m10}) - \lambda_2(\Phi^j_{m2i} - \Phi^j_{m20})}{\lambda_2^2 - \lambda_1^2}\right)\right\} \quad \text{(A-18)}$$

Though it would be possible to use Equation (A-4) and its L_2 equivalent to find the PPS solution for the demonstration, smoothing with the phase observations, as in Equation (A-18), is a better approach. The only problem is that phase jumps need to be found and appropriate action taken.

Interruptions in the phase observations may be identified by cycle slips or by actual time gaps in the observations for a given satellite. Time gaps in the observations will be obvious, but the identification of cycle slips is more difficult. In order to detect cycle slips in the phase data and also to improve the pseudorange observations, the observations between time epochs can be differenced. A cycle slip is a phenomenon that occurs when the receiver mistracks the satellite signal without losing lock (no time gap) and adds or subtracts some multiple of an integer (or half integer, depending upon the receiver design) to the phase observation. Since this occurrence adds or subtracts a wavelength (or more) of range between the receiver antenna and the satellite, an erroneous position solution will result if it remains undetected.

PHASE JUMP DETECTION

Occasionally the receiver may slip or jump cycles when recording the phase observations while tracking a satellite. If this occurs, the resulting average pseudorange, computed from Equation (A-18), will be in error. In order to prevent this problem, the raw phase observations need to be checked for consistency. This can be accomplished through the use of Equation (A-14). The expression on the left of the equals sign in Equation (A-14) differences the difference between the phase at the current time and the phase at a given epoch between the two frequencies. Each phase difference is converted to units of meters by multiplying by the appropriate wavelength. As the right-hand side of the equation shows, this is a measure of the change in the ionospheric path length from site m to satellite j from the epoch time to the current time as the satellite moves across the sky. Generally, this change is very smooth; in fact, if there were no ionosphere, the right-hand side of the equation would be zero.

A single cycle phase jump in Φ^j_{m1i} or Φ^j_{m2i} shows up as a wavelength step in the smooth change due to the ionosphere. This jump should be easily detectable if it occurs. Since either or both phases may jump at the same time, the minimum jump magnitudes include the following possibilities: $\pm\lambda_1$, $\pm\lambda_2$, $\lambda_1 \pm \lambda_2$, or $\lambda_2 \pm \lambda_1$. Figure A-2 shows an example of Equation (A-14) for a short span of observations with no jumps recorded. Figure A-3 shows the same data span with several single wavelength jumps artificially included in the observations. PRN03 illustrates a positive λ_1 jump. PRN14 illustrates a positive λ_2 jump. PRN18 illustrates a jump of the sum $\lambda_1 + \lambda_2$; PRN22 illustrates a jump of the difference $\lambda_2 - \lambda_1$; and PRN25 illustrates a jump of the difference $\lambda_1 - \lambda_2$. PRN28 and PRN29 exhibit no change. The least obvious jump is the jump with the smallest magnitude, the $\lambda_1 + \lambda_2$ case. This is about 5 cm, which is equal to the difference in wavelength (24-19 cm). Usually, even this small jump should be detectable.

The procedure proposed to deal with these jumps is as follows. Fit a polynomial to the computation on the left-hand side of Equation (A-14) for each satellite. The degree of the polynomial required will depend upon the time interval between observations and the dynamics of the geometry change between the satellite and the site. For most cases, a linear polynomial of the form illustrated in Equation (A-19) will suffice.

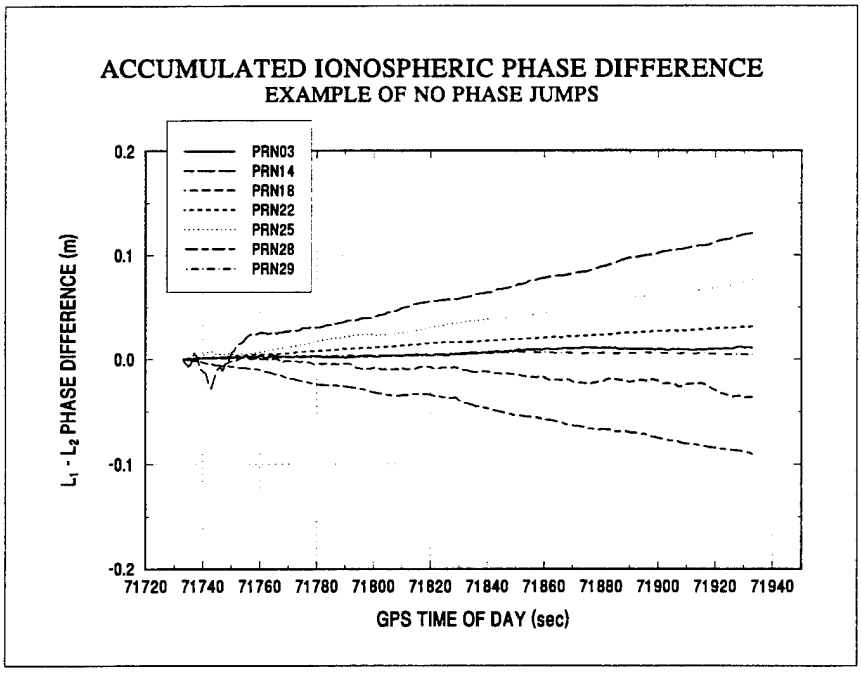

FIGURE A-2. AN EXAMPLE OF EQUATION (A-14) WITH NO JUMPS

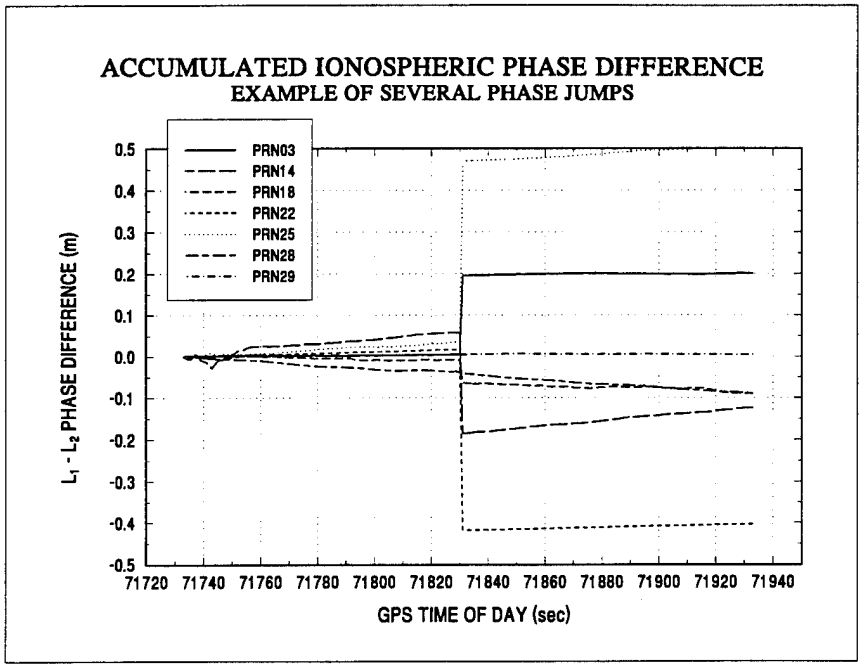

FIGURE A-3. ARTIFICIAL PHASE JUMPS INSERTED INTO THE DATA

$$\lambda_1(\phi^j_{m1i} - \phi^j_{m10}) - \lambda_2(\phi^j_{m2i} - \phi^j_{m20}) = a_0 + a_1(t_i - t_0) \quad \text{(A-19)}$$

A minimum of two observations is needed to evaluate the two coefficients. Perform a sliding fit over the last 300 sec of data or at least two observations, whichever is longer. If a jump occurred at the current time, t_i, it should be readily evident by evaluating the residuals of the fit (the difference between the polynomial evaluated at t_i and the phase difference observation at that time). If this residual exceeds the ±5 cm minimum, then the pseudorange smoothing must be restarted for this satellite. That means the sum in Equation (A-18) is ended and all the pseudoranges up to the current time, evaluated using Equation (A-17). The reference time t_0 is then reset to the current time and a new sum begun.

COMPUTE SATELLITE POSITION

The satellite position will ultimately be computed with both the broadcast ephemerides and the DMA precise ephemerides. Both are Earth-Centered, Earth-Fixed (ECEF) and need to be evaluated to obtain the satellite position at the time of transmission. The procedure for doing this is described in this section.

BROADCAST EPHEMERIS

The broadcast ephemerides from each satellite in view are available in the RINEX file format. A satellite position at the time of transmission is required in order to compute the range along the line from the receiving antenna to the transmitting antenna. Each observed pseudorange and phase measurement is tagged with the local time of reception determined by each receiver. All received epochs from different sites at the same time will have the same time tag, but the true time of reception at each site will be in error by an unknown receiver offset. The times of transmission from a given satellite will be different for each receiver since each is at a different range from that satellite. The true time of transmission for each satellite at each receiver must be found through an iterative process. This will be described later.

Once the time of transmission is known, the satellite's ECEF position is found by evaluating a series of equations with coefficients obtained from the current ephemeris. The equations are repeated below.[A-4]

WGS84 CONSTANTS

Universal gravitational constant times the mass of the Earth: $\mu = 3.986005\times10^{14}$ m^3/s^2

Earth's rotation rate: $\dot{\Omega}_e = 7.2921151467\times10^{-5}$ rad/s

Speed of light in vacuum: c = 299792458 m/s

Relativistic constant: $F = -4.442809305\times10^{-10}$ s/m^{½}

EPHEMERIS PARAMETERS INCLUDED IN THE BROADCAST MESSAGE

Mean anomaly at the reference time	M_0
Mean motion difference	Δn
Eccentricity	e
Semimajor axis square root	$a^{1/2}$
Right ascension at reference time	Ω_0
Inclination at reference time	i_0
Argument of perigee	ω
Rate of right ascension	$\dot{\Omega}$
Rate of inclination	i_{dot}
Cosine harmonic for argument of latitude	C_{uc}
Sine harmonic for argument of latitude	C_{us}
Cosine harmonic for orbit radius	C_{rc}
Sine harmonic for orbit radius	C_{rs}
Cosine harmonic for inclination	C_{ic}
Sine harmonic for inclination	C_{is}
Reference time ephemeris	t_{oe}

EQUATIONS FOR COMPUTATION OF THE SATELLITE POSITION

Semimajor axis of the Earth	$a = (\sqrt{a})^2$
Computed mean motion	$n_0 = \sqrt{\frac{\mu}{a^3}}$
Time from ephemeris reference epoch	$t_k = t - t_{oe}$
Corrected mean motion	$n = n_0 + \Delta n$
Mean anomaly	$M_k = M_0 + n\,t_k$
Eccentric anomaly	$E_k = M_k + e \sin E_k$

Since the eccentric anomaly E_k appears on left of the equals sign in the equation above and also on the right as the argument of a sine function, it must be solved by iteration. Start with $E_k \approx M_k$ on the right and compute a new E_k. Continue iterating until the new E_k differs from the previous by less than 10^{-9} radians or four iterations, whichever comes first.

True anomaly	$v_k = \tan^{-1}\left[\frac{\sqrt{1 - e^2}\sin E_k}{\cos E_k - e}\right]$
Argument of latitude	$\phi_k = v_k + \omega$
Argument of latitude correction	$\delta u_k = C_{us}\sin 2\phi_k + C_{uc}\cos 2\phi_k$
Radius correction	$\delta r_k = C_{rc}\cos 2\phi_k + C_{rs}\sin 2\phi_k$
Inclination correction	$\delta i_k = C_{ic}\cos 2\phi_k + C_{is}\sin 2\phi_k$
Corrected argument of latitude	$u_k = \phi_k + \delta u_k$
Corrected radius	$r_k = a(1 - e\cos E_k) + \delta r_k$
Corrected inclination	$i_k = i_0 + \delta i_k + i_{dot}\,t_k$

Positions in the orbital plane	$\dot{x}_k = r_k \cos u_k$ $\dot{y}_k = r_k \sin u_k$
Corrected longitude of ascending node	$\Omega_k = \Omega_0 + (\dot{\Omega} - \dot{\Omega}_e) t_k - \dot{\Omega}_e t_{oe}$
Earth fixed coordinates	$x_k = \dot{x}_k \cos \Omega_k - \dot{y}_k \cos i_k \sin \Omega_k$ $y_k = \dot{x}_k \sin \Omega_k + \dot{y}_k \cos i_k \cos \Omega_k$ $z_k = \dot{y}_k \sin i_k$
Satellite clock correction	$\Delta t_o^j = a_0 + a_1 (t - t_{oc}) + a_2 (t - t_{oc})^2 + \Delta t_r^j$
Relativistic correction	$\Delta t_r^j = F e \sqrt{a} \sin E_k$

Test the values of $t - t_{oe}$ and $t - t_{oc}$ in the following way. If either difference is greater than 302,400 sec, subtract 604,800. If either difference is less than -302,400, add 604,800.

PRECISE EPHEMERIS

The precise satellite ephemerides and clock corrections are available in an OMNIS file format[A-5] for each 15-min epoch during the 8-day fit span. Each satellite ephemeris file contains the GPS time of week and the ECEF satellite position and velocity at that time. To evaluate the satellite position at other times, an eight-point Lagrange interpolation routine is normally used. The separate clock file contains the satellite clock time offsets for all the satellites at 15-min epochs. These time offsets can be used directly (after changing the units to seconds) for $\tau^j_{..i}$ in Equation (A-4).

The second record of the clock file contains a list of satellite jumps that occur during the period covered by the ephemerides. Since an interpolation routine will give erroneous values when it tries to interpolate across a jump, a satellite with a jump within the time interval to be processed cannot be used. Therefore, before beginning any processing, check the precise clock file for satellite clock jumps between the start time ($t_1 - t_I$) and stop times ($t_n + t_I$) listed on the configuration file. The value of t_I is the extra number of seconds needed to accommodate the width of the interpolating function. If such jumps exist, print a message to the user and then add that PRN number to the list of satellites to be omitted (also listed on the configuration file).

The DMA precise ephemerides gives the location of the center of mass of the GPS satellites, whereas the observations are, by definition, referenced to the phase center of the transmitting antenna. The phase center and the center of mass are different points, and a correction must be added to account for this difference. No corresponding correction is needed for the broadcast ephemerides because it is already referenced to the satellite antenna phase center.[A-6] An algorithm developed to compute this correction follows.[A-7]

First, the position vectors of the sun and the satellite need to be known at the time of interest. The satellite position vector is obtained from the precise ephemeris in the usual way, but the position vector of the sun must be converted from inertial space. Two subroutines to perform this task are SUNPOS and HAA. The first computes the sun's position in inertial space, and the second transforms it into ECEF coordinates. Given these two vectors: $\boldsymbol{r}_o$, the ECEF vector for the sun, and $\boldsymbol{r}^j_{..i}$, the ECEF vector for the satellite, the unit vectors for a body-centered coordinate system can be computed. It is known that the GPS antennas always must point toward the earth. This axis is the

z body axis $\hat{z}_B$, and is coincident with, but in the opposite direction to, the satellite vector $\boldsymbol{r}^j_{.i}$. It is also known that the solar panels, the y body axis, must be perpendicular to the earth-sun vector. The x body axis completes a right handed system. The relationships are shown in the following set of equations.

$$\hat{z}_B = -\frac{\boldsymbol{r}^j_{.i}}{\left|\boldsymbol{r}^j_{.i}\right|}$$

$$\hat{y}_B = \frac{\left(\boldsymbol{r}^j_{.i} \times \boldsymbol{r}_o\right)}{\left|\boldsymbol{r}^j_{.i} \times \boldsymbol{r}_o\right|} \qquad \text{(A-20)}$$

$$\hat{x}_B = \hat{y}_B \times \hat{z}_B$$

These body-centered unit vectors are expressed in terms of the ECEF coordinates in Equation (A-20). For Block II satellites, the antenna phase center lies at {0.279, 0, 1.943} in the body-centered system. Therefore the vector to be added to the satellite vector $\boldsymbol{r}^j_{.i}$ (the range decreases) is given in Equation (A-21) using the unit vectors given in Equation (A-20).

$$\Delta \boldsymbol{r}^j = x_B \hat{x}_B + y_B \hat{y}_B + z_B \hat{z}_B \qquad \text{(A-21)}$$

SATELLITE POSITION AT THE TIME OF TRANSMISSION

Let t_R be the GPS time of reception (seconds of the week at epoch i) as read from the RINEX file containing the data observed at a given site. The ECEF position of the satellite at the time of transmission can be computed using the equations listed above. In order to find the propagation path length, the position of the satellite at the time of transmission t_T is required. The expression defining the propagation path from the user located at $\boldsymbol{r}_{m.i}$ to the satellite at $\boldsymbol{r}^j_{.i}$ is given in Equation (A-22). This is Equation (A-6) with the GPS times of signal transmission t_T and signal reception t_R written explicitly.

$$\boldsymbol{r}^j_{m.i}(t_R) = \boldsymbol{r}^j_{.i}(t_T) - \boldsymbol{r}_{m.i}(t_R) \qquad \text{(A-22)}$$

Since the observation time tags are at t_R, this frame of reference will be chosen as the earth-fixed frame at t_R. This allows the station position vector to be fixed and defined as shown in Equation (A-23).

$$\boldsymbol{r}_{m.i}(t_R) = x_{m.i}\hat{x} + y_{m.i}\hat{y} + z_{m.i}\hat{z} \qquad \text{(A-23)}$$

The time of transmission is unique for each satellite (subscript j) and must be computed starting from the time of reception. The GPS time of transmission is found by subtracting the propagation path delay from the time of reception and including the correction for the satellite clock offset. This is shown in Equation (A-24).

$$t_T^j \approx t_R - \frac{r_{mi}^j(t_R^j)}{c} - \Delta t_o^j \qquad \text{(A-24)}$$

Since the time of transmission appears on both sides of the equation (see Equation (A-20)), some iteration will be required. For the first trial, the propagation term $\frac{r_{mi}^j(t_R^j)}{c}$ can be approximated by 0.075 sec, and Δt_o^j, the satellite clock correction, by zero. This will give a transmission time to use in the ephemeris computations and allow a satellite vector and a clock correction to be found. Since this is an ECEF computation, the satellite position is computed in the frame at the time of transmission. This result needs to be rotated into the frame at the time of reception so that both vectors are known in a common frame. Then the subtraction shown in Equation (A-22) can be performed.

$$\begin{aligned} x_R^j &= x_T^j \cos(\theta) + y_T^j \sin(\theta) \\ y_R^j &= -x_T^j \sin(\theta) + y_T^j \cos(\theta) \\ z_R^j &= z_T^j \end{aligned} \qquad \text{(A-25)}$$

The transformation, shown in Equation (A-25), just rotates the ECEF frame around the z axis to compensate for the rotation of the earth during the time it took the signal to travel from the particular satellite j to the receiver antenna. The value of the angle is shown in Equation (A-26). Continue to iterate Equations (A-24) and (A-25), by computing a new satellite vector and clock offset, until the change in θ from one iteration to the next is less than a microradian.

$$\theta = \dot{\Omega}_E \frac{r_{mi}^j(t_R)}{c} \qquad \text{(A-26)}$$

$$\dot{\Omega}_E = \dot{\Omega}_e = 7.2921151467 \times 10^{-5} \ rad/s \qquad \text{(A-27)}$$

TROPOSPHERIC REFRACTION MODEL

Tropospheric refraction is caused by the variation of the index of refraction from that of free space as a result of the molecules in the atmosphere. This causes a delay and a bending of the ray path as it propagates through the atmosphere along the line of sight from the satellite to the receiving antenna. This refraction is independent of frequency and cannot be eliminated by the dual frequencies transmitted by the GPS satellites; instead it must be modeled. The index of refraction is a function

of environmental conditions in the atmosphere, most prominently by temperature, pressure, and humidity. The total delay is dependent upon the propagation path length, which in turn depends upon the elevation angle $\epsilon^{j}_{m.i}$ of satellite j as seen from site m at time t_i. The model proposed here follows Goad.[A-8]

The local vertical in ECEF coordinates can be computed from the site longitude $\gamma_{m.i}$ and latitude $\beta_{m.i}$ as given by Equation (A-28).

$$\hat{u}_{m.i} = \cos \beta_{m.i} \cos \lambda_{m.i} \hat{x} + \cos \beta_{m.i} \sin \lambda_{m.i} \hat{y} + \sin \beta_{m.i} \hat{z} \qquad \text{(A-28)}$$

The elevation angle can be computed from the angle between the local vertical $\hat{u}_{m.i}$ and the site-to-satellite vector $r^{j}_{m.i}$ as shown in Equation (A-29).

$$\epsilon^{j}_{m.i} = \frac{\pi}{2} - Arccos \left(\hat{r}^{j}_{m.i} \cdot \hat{u}_{m.i} \right) \qquad \text{(A-29)}$$

There are two components in the tropospheric model: the dry and the wet. The total delay is the sum of the two. There are various parts to the complete formula and these are listed below for the two components. Temperature, T, is in degrees Kelvin; humidity, H, is in percent; and pressure, P, is in millibars.

DRY COMPONENT (SUBSCRIPT 0)

Surface refractivity: $$N_{0\,m.i} = 77.624 \frac{P_{m.i}}{T_{m.i}}$$

Height of tropopause (dry): $$h_{0\,m.i} = \frac{5\,(0.002277\ P_{m.i})}{N_{0\,m.i} \times 10^{-6}}$$

WET COMPONENT (SUBSCRIPT 1)

Temperature scale: $$a_{T\,m.i} = \frac{7.5\,(T_{m.i} - 273.15)}{237.3 + (T_{m.i} - 273.15)}$$

Water vapor pressure: $$w_{m.i} = \frac{H_{m.i}}{100} \times 6.11 \times 10^{a_{T\,m.i}}$$

Surface refractivity: $$N_{1\,m.i} = -12.92 \frac{w_{m.i}}{T_{m.i}} + 371900 \frac{w_{m.i}}{T^2_{m.i}}$$

Height of tropopause (wet): $$h_{1\,m.i} = \frac{5\,(0.002277)}{N_{1\,m.i} \times 10^{-6}} \left(\frac{1255}{T_{m.i}} + 0.05 \right) w_{m.i}$$

EXPANSION FACTORS

Range to tropopause $$r^{j}_{\xi\,m.i} = \sqrt{(a_e + h_{\xi\,m.i})^2 - (a_e \cos \epsilon^{j}_{m.i})^2} - a_e \sin \epsilon^{j}_{m.i}$$

Where the semimajor axis $a_e = 6378137$ m

Factor a_ξ

$$a^{j}_{\xi m.i} = - \frac{\sin \epsilon^{j}_{m.i}}{h_{\xi m.i}}$$

Factor b_ξ

$$b^{j}_{\xi m.i} = - \frac{\cos^2 \epsilon^{j}_{m.i}}{2\, h_{\xi m.i}\, a_e}$$

EXPANSION TERMS

Term α_1 $\quad \alpha_{1,\xi} = 1$

Term α_2 $\quad \alpha_{2,\xi} = 4\, a_{\xi m.i}$

Term α_3 $\quad \alpha_{3,\xi} = 6\, a^{2}_{\xi m.i} + 4\, b_{\xi m.i}$

Term α_4 $\quad \alpha_{4,\xi} = 4\, a_{\xi m.i} (a^{2}_{\xi m.i} + 3\, b_{\xi m.i})$

Term α_5 $\quad \alpha_{5,\xi} = a^{4}_{\xi m.i} + 12\, a^{2}_{\xi m.i} b_{\xi m.i} + 6\, b^{2}_{\xi m.i}$

Term α_6 $\quad \alpha_{6,\xi} = 4\, a_{\xi m.i} b_{\xi m.i} (a^{2}_{\xi m.i} + 3 b_{\xi m.i})$

Term α_7 $\quad \alpha_{7,\xi} = b^{2}_{\xi m.i} (6\, a^{2}_{\xi m.i} + 4\, b_{\xi m.i})$

Term α_8 $\quad \alpha_{8,\xi} = 4\, a_{\xi m.i} b^{3}_{\xi m.i}$

Term α_9 $\quad \alpha_{9,\xi} = b^{4}_{\xi m.i}$

SUM OF DRY AND WET TERMS

The tropospheric refraction range correction at each observation is given by Equation (A-30).

$$T^{j}_{m.i} = 10^{-6} \sum_{\xi = 0}^{1} N_{\xi m.i} \left[\alpha_{1,\xi}\, r^{j}_{\xi m.i} + \frac{\alpha_{2,\xi}}{2} (r^{j}_{\xi m.i})^2 + \ldots + \frac{\alpha_{9,\xi}}{9} (r^{j}_{\xi m.i})^9 \right] \qquad \text{(A-30)}$$

THE NAVIGATION SOLUTION

At each time of observation, a computed observation from the receiver antenna to the satellites in view must be computed. This computed observation, plus the first term of the Taylor series expansion, constitutes a linear approximation to the observations, as was shown in Equation (A-1). For single-frequency pseudorange, the computed observation (C_0 in Equation (A-1)) consists of the terms listed in Equation (A-4). However, since two-frequency data are available, the ionospheric term can be removed from the observations, as was described in the discussion leading to Equation (A-17). Therefore, the computed observation has the same form as Equation (A-4) except that the ionospheric term is deleted. The computed observation is rewritten as Equation (A-31).

$$\rho^{j}_{mIi} = \tilde{r}^{j}_{m.i} + \gamma^{j}_{m.i} + c\, (\tilde{\tau}_{m.i} - \tau^{j}_{..i}) + T^{j}_{m.i} + SA^{\,j}_{..i} \qquad \text{(A-31)}$$

The first term on the right in Equation (A-31) is the geometric range computed from Equation (A-6) and shown in Equation (A-32).

$$\tilde{r}^{j}_{m.i} = \sqrt{(x^{j}_{.i} - \tilde{x}_{m.i})^2 + (y^{j}_{.i} - \tilde{y}_{m.i})^2 + (z^{j}_{.i} - \tilde{z}_{m.i})^2} \qquad \text{(A-32)}$$

A guess for the receiver antenna position (indicated by the tilde) is required in order to compute this range. The second term on the right is the periodic relativity contribution, which is computed as part of the satellite ephemerides. The third term consists of the two clock offsets. The satellite clock offset is known from the satellite ephemerides, while the local offset is unknown (set to zero in Equation (A-31)) and must be included in the state vector along with corrections to the antenna position. The fourth term is the tropospheric delay and is modeled as described in a previous section. Finally, there are the SA effects, which are known in a true PPS solution, but will remain unknown for this demonstration and are ignored.

PARTIAL DERIVATIVES

In a navigation solution, the state vector (ΔX_0 in Equation (A-1)) consists of four elements: the corrections to the antenna position $\Delta x_{m.i}$, $\Delta y_{m.i}$, $\Delta z_{m.i}$, and the clock offset $\Delta\tau_{m.i}$. The partial derivative matrix is constructed from the partial derivative of each term in Equation (A-31) with respect to each state element. This matrix will be rectangular, having four columns (one for each state) and $n_{O\,m.i}$ rows, where $n_{O\,m.i}$ is the number of observations (equal to the number of satellites being tracked) from the receiver at site m at time t_i. In order to perform the navigation solution, at least four satellite observations are needed, $n_{O\,m.i} \geq 4$.

The partial of $\rho^{j}_{m.i}$ with respect to $x_{m.i}$: $$\frac{\partial \tilde{\rho}^{j}_{m.i}}{\partial \tilde{x}_{m.i}} = \frac{x_{m.i} - \tilde{x}^{j}_{.i}}{\tilde{r}^{j}_{m.i}}$$

The partial of $\rho^{j}_{m.i}$ with respect to $y_{m.i}$: $$\frac{\partial \tilde{\rho}^{j}_{m.i}}{\partial \tilde{y}_{m.i}} = \frac{y_{m.i} - \tilde{y}^{j}_{.i}}{\tilde{r}^{j}_{m.i}}$$

The partial of $\rho^{j}_{m.i}$ with respect to $z_{m.i}$: $$\frac{\partial \tilde{\rho}^{j}_{m.i}}{\partial \tilde{z}_{m.i}} = \frac{z_{m.i} - \tilde{z}^{j}_{.i}}{\tilde{r}^{j}_{m.i}}$$

The partial of $\rho^{j}_{m.i}$ with respect to $c\tau_{m.i}$: $$\frac{\partial \tilde{\rho}^{j}_{m.i}}{\partial\, c\,\tilde{\tau}_{m.i}} = 1$$

Equation (1) can be rewritten in matrix form with each element explicitly indicated as follows:

$$\begin{bmatrix} \rho^{1}_{m.i} \\ \rho^{2}_{m.i} \\ \rho^{3}_{m.i} \\ \cdots \\ \rho^{j}_{m.i} \end{bmatrix}_{O} = \begin{bmatrix} \tilde{\rho}^{1}_{m.i} \\ \tilde{\rho}^{2}_{m.i} \\ \tilde{\rho}^{3}_{m.i} \\ \cdots \\ \tilde{\rho}^{j}_{m.i} \end{bmatrix}_{C} + \begin{bmatrix} \frac{\partial \tilde{\rho}^{1}_{m.i}}{\partial \tilde{x}_{m.i}} & \frac{\partial \tilde{\rho}^{1}_{m.i}}{\partial \tilde{y}_{m.i}} & \frac{\partial \tilde{\rho}^{1}_{m.i}}{\partial \tilde{z}_{m.i}} & \frac{\partial \tilde{\rho}^{1}_{m.i}}{\partial \tilde{\tau}_{m.i}} \\ \frac{\partial \tilde{\rho}^{2}_{m.i}}{\partial \tilde{x}_{m.i}} & \frac{\partial \tilde{\rho}^{2}_{m.i}}{\partial \tilde{y}_{m.i}} & \frac{\partial \tilde{\rho}^{2}_{m.i}}{\partial \tilde{z}_{m.i}} & \frac{\partial \tilde{\rho}^{2}_{m.i}}{\partial \tilde{\tau}_{m.i}} \\ \frac{\partial \tilde{\rho}^{3}_{m.i}}{\partial \tilde{x}_{m.i}} & \frac{\partial \tilde{\rho}^{3}_{m.i}}{\partial \tilde{y}_{m.i}} & \frac{\partial \tilde{\rho}^{3}_{m.i}}{\partial \tilde{z}_{m.i}} & \frac{\partial \tilde{\rho}^{3}_{m.i}}{\partial \tilde{\tau}_{m.i}} \\ \cdots & \cdots & \cdots & \cdots \\ \frac{\partial \tilde{\rho}^{j}_{m.i}}{\partial \tilde{x}_{m.i}} & \frac{\partial \tilde{\rho}^{j}_{m.i}}{\partial \tilde{y}_{m.i}} & \frac{\partial \tilde{\rho}^{j}_{m.i}}{\partial \tilde{z}_{m.i}} & \frac{\partial \tilde{\rho}^{j}_{m.i}}{\partial \tilde{\tau}_{m.i}} \end{bmatrix} \cdot \begin{bmatrix} \Delta x_{m.i} \\ \Delta y_{m.i} \\ \Delta z_{m.i} \\ \Delta \tau_{m.i} \end{bmatrix} \tag{A-33}$$

LEAST SQUARES MATRIX SOLUTION

Returning to the notation of Equation (A-1), the solution for the state vector proceeds as follows. Form the difference between the observed ranges and the computed ranges as in Equation (A-34).

$$\frac{\partial C}{\partial X} \Delta X = O - C \tag{A-34}$$

Next introduce a *weight* matrix, W, which will (for now) be an $n_{O\,m.i} \times n_{O\,m.i}$ identity matrix, where $n_{O\,m.i} = j$, the number of satellites. Then, pre-multiply both sides by the transpose of the matrix of partials times the weight matrix as shown in Equation (A-35). With an identity weight matrix, it is assumed that all observations have equal weight.

$$\left[\left(\frac{\partial C}{\partial X} \right)^{T} W \frac{\partial C}{\partial X} \right] \Delta X = \left(\frac{\partial C}{\partial X} \right)^{T} W (O - C) \tag{A-35}$$

The final step is to isolate the ΔX on the left by pre-multiplying both sides by the inverse of the matrix quantity in brackets in Equation (A-35). This result is shown in Equation (A-36).

$$\Delta X = \left[\left(\frac{\partial C}{\partial X} \right)^{T} W \frac{\partial C}{\partial X} \right]^{-1} \left(\frac{\partial C}{\partial X} \right)^{T} W (O - C) \tag{A-36}$$

The navigation solution, at the time of the observations at t_i, is shown in Equation (A-37). It is the sum of the guessed position ($\tilde{x}_{m.i}$, $\tilde{y}_{m.i}$, $\tilde{z}_{m.i}$) and the deltas from the state vector in Equation (A-36).

$$\begin{aligned} \hat{x}_{m.i} &= \tilde{x}_{m.i} + \Delta x_{m.i} \\ \hat{y}_{m.i} &= \tilde{y}_{m.i} + \Delta y_{m.i} \\ \hat{z}_{m.i} &= \tilde{z}_{m.i} + \Delta z_{m.i} \\ \hat{\tau}_{m.i} &= \Delta \tau_{m.i} \end{aligned} \qquad \text{(A-37)}$$

The results from Equation (A-37) can be used to compute an adjusted computed observation vector from Equation (A-31). This adjusted vector, $\hat{\rho}^j_{m.i}$, when subtracted from the original observations, should have a near-zero RSS of the mean. The standard deviation of the difference gives an estimate of the error in the solution.

In the absence of SA (dither), Equation (A-37) would be the equivalent PPS solution that must be saved. However, the dither needs to be eliminated from the test data set. This can be approximated by solving for the instantaneous satellite clock offset in a separate dither estimator program.

DIFFERENTIAL CORRECTION FOR RANGE BIAS ESTIMATION

In order to estimate the dither on the satellite clocks at each observation time, at least two static sites, with known positions, observing simultaneously, are needed. Assuming independent solutions, the reason for this is as follows. Each site observes k satellites, each of which has an instantaneous range bias due to dither. Thus, there are k unknowns. If the station position and clock offset are known, the dither could be solved, but the site clock is not known well enough. It must be included in the list of unknowns, making $k+1$. A second site observes the same satellites and adds only its clock to the list of unknowns. Therefore, in general, for l sites observing k satellites simultaneously, there will be kl observations and $k+l$ unknowns. For $k>3$, and two sites, $2k$ is greater than $k+2$. Two sites whose positions are known will be enough to estimate the k dither and two local clock range biases.

The observation equations for the dither estimator are shown in Equation (A-38). It is assumed that the site positions are static and known. The unknowns will be the two site clock offsets, $\tau_{m.i}, \tau_{n.i}$, and the corrections to the satellite clock predictions found in the broadcast ephemerides, $\tau^j_{..i} + \delta\tau^j_{..i}$, where $1 \le j \le k$.

$$\begin{aligned} \tilde{\rho}^j_{m.i} &= r^j_{m.i} + \gamma^j_{m.i} + c\,(\tilde{\tau}_{m.i} - \tau^j_{..i} - \delta\tau^j_{..i}) + T^j_{m.i} \\ \tilde{\rho}^j_{n.i} &= r^j_{n.i} + \gamma^j_{n.i} + c\,(\tilde{\tau}_{n.i} - \tau^j_{..i} - \delta\tau^j_{..i}) + T^j_{n.i} \end{aligned} \qquad \text{(A-38)}$$

Dither Partials

The partials derivatives are as follows:

The partial of $\rho^j_{m.i}$ with respect to $c\,\tau_{m.i}$: $\dfrac{\partial \rho^j_{m.i}}{\partial\, c\,\tau_{m.i}} = 1$

The partial of $\rho^j_{m.i}$ with respect to $c\,\delta\tau^j_{..i}$ $\dfrac{\partial \rho^j_{m.i}}{\partial (c\,\delta\tau_{m.i})} = -1$

Similar partials apply for site *n* and the other satellites. The solution matrix is similar to that in the navigation solution described above. The matrix equation analogous to Equation (A-33) is shown in Equation (A-39) below. The satellite dither solutions should be written to a file and saved for use in the PPS navigation solution. The file should include the GPS time of week, the week number, and the satellite PRN numbers with their respective dither corrections. The PPS program then adds these corrections to the clock predictions obtained from the broadcast ephemerides at the particular time of the observation. This process approximates the dither removal that would be performed in the field by other means to obtain the PPS solution.

$$\begin{bmatrix} \rho^{1}_{m.i} \\ \rho^{2}_{m.i} \\ \rho^{3}_{m.i} \\ \cdots \\ \rho^{j}_{m.i} \\ \rho^{1}_{n.i} \\ \rho^{2}_{n.i} \\ \rho^{3}_{n.i} \\ \cdots \\ \rho^{j}_{n.i} \end{bmatrix}_{O} = \begin{bmatrix} \tilde{\rho}^{1}_{m.i} \\ \tilde{\rho}^{2}_{m.i} \\ \tilde{\rho}^{3}_{m.i} \\ \cdots \\ \tilde{\rho}^{j}_{m.i} \\ \tilde{\rho}^{1}_{n.i} \\ \tilde{\rho}^{2}_{n.i} \\ \tilde{\rho}^{3}_{n.i} \\ \cdots \\ \tilde{\rho}^{j}_{n.i} \end{bmatrix}_{C} + \begin{bmatrix} \frac{\partial \tilde{\rho}^{1}_{m.i}}{\partial c\tilde{\tau}_{m.i}} & 0 & \frac{\partial \tilde{\rho}^{1}_{m.i}}{\partial c\delta\tilde{\tau}^{1}_{..i}} & 0 & 0 & \cdots & 0 \\ \frac{\partial \tilde{\rho}^{2}_{m.i}}{\partial c\tilde{\tau}_{m.i}} & 0 & 0 & \frac{\partial \tilde{\rho}^{2}_{m.i}}{\partial c\delta\tilde{\tau}^{2}_{..i}} & 0 & \cdots & 0 \\ \frac{\partial \tilde{\rho}^{3}_{m.i}}{\partial c\tilde{\tau}_{m.i}} & 0 & 0 & 0 & \frac{\partial \tilde{\rho}^{3}_{m.i}}{\partial c\delta\tilde{\tau}^{3}_{..i}} & \cdots & 0 \\ \cdots & \cdots & \cdots & \cdots & \cdots & \cdots & \cdots \\ \frac{\partial \tilde{\rho}^{j}_{m.i}}{\partial c\tilde{\tau}_{m.i}} & 0 & 0 & 0 & 0 & \cdots & \frac{\partial \tilde{\rho}^{j}_{m.i}}{\partial c\delta\tilde{\tau}^{j}_{..i}} \\ 0 & \frac{\partial \tilde{\rho}^{1}_{n.i}}{\partial c\tilde{\tau}_{n.i}} & \frac{\partial \tilde{\rho}^{1}_{n.i}}{\partial c\delta\tilde{\tau}^{1}_{..i}} & 0 & 0 & \cdots & 0 \\ 0 & \frac{\partial \tilde{\rho}^{2}_{n.i}}{\partial c\tilde{\tau}_{n.i}} & 0 & \frac{\partial \tilde{\rho}^{2}_{n.i}}{\partial c\delta\tilde{\tau}^{2}_{..i}} & 0 & \cdots & 0 \\ 0 & \frac{\partial \tilde{\rho}^{3}_{n.i}}{\partial c\tilde{\tau}_{n.i}} & 0 & 0 & \frac{\partial \tilde{\rho}^{3}_{n.i}}{\partial c\delta\tilde{\tau}^{3}_{..i}} & \cdots & 0 \\ \cdots & \cdots & \cdots & \cdots & \cdots & \cdots & \cdots \\ 0 & \frac{\partial \tilde{\rho}^{j}_{n.i}}{\partial c\tilde{\tau}_{n.i}} & 0 & 0 & 0 & \cdots & \frac{\partial \tilde{\rho}^{j}_{n.i}}{\partial c\delta\tilde{\tau}^{j}_{..i}} \end{bmatrix} \cdot \begin{bmatrix} \Delta c\tau_{m.i} \\ \Delta c\tau_{n.i} \\ \Delta c\tau^{1}_{..i} \\ \Delta c\tau^{2}_{..i} \\ \Delta c\tau^{3}_{..i} \\ \cdots \\ \Delta c\tau^{j}_{..i} \end{bmatrix} \quad \text{(A-39)}$$

As it stands, the problem as formulated by Equation (A-39) is ill-conditioned and cannot be solved. In order to fix this, one satellite was chosen to be deweighted: in effect, given a zero range bias. This provides a reference with which the other ranged biases may be compared. Therefore, the solutions are satellite range biases with respect to the reference. The desired range correction is still accomplished, since the navigation solutions treat common biases as local clock biases. If the true local clock bias is of no interest, this method can be used to remove the dither effect from the pseudoranges.

CONVERT THE PPS SOLUTION USING THE PRECISE EPHEMERIDES

With the PPS solution in hand, the next task is to improve it by using the DMA precise ephemerides and clock estimates to replace the broadcast ephemerides predictions. To do this, both ephemerides are required, as well as the knowledge about which particular satellites were tracked at each PPS navigation solution.

FORM THE COMPUTED OBSERVATION FROM THE BROADCAST EPHEMERIDES

At each PPS solution time, form the computed observation from the PPS solution and the broadcast ephemerides in the same manner as was described previously; see text preceeding Equation (A-31). Since the data that produced the PPS solution for this demonstration are known, use the same set of satellites that were used at each observation to obtain the PPS solution. The PPS solution and the broadcast ephemerides will generate the vector corresponding to C_b in Equation (A-3).

FORM THE COMPUTED OBSERVATION FROM THE PRECISE EPHEMERIDES

Evaluate the precise ephemerides and satellite clock offsets at the same observation times as the broadcast ephemerides above. Use the eight-point Lagrange interpolation and iteration scheme to find the time of transmission for each satellite. Also, use the PPS solutions for the antenna site positions when evaluating Equation (A-31). The result of this will be the vector corresponding to C_p in Equation (A-3).

The relativity correction needs to be computed separately and added to the satellite clock offset in the same manner as with the broadcast ephemerides. However, since the precise ephemerides deals with ECEF positions and velocities rather than orbit elements, the computation of relativity cannot use the same equation as was used with the broadcast ephemerides. An equivalent form is given in the equation below where r and v are the satellite's ECEF position and velocity at time t_i.[A-9]

$$\Delta t_r^j = \frac{2}{c} \mathbf{r}_{.i}^j \cdot \mathbf{v}_{.i}^j \qquad \text{(A-40)}$$

FORM THE PARTIAL DERIVATIVES

The partial derivatives will have the same form as in the PPS solution described previously. Use the computed value from the precise ephemerides to evaluate $\rho^j_{m.i}$ and its components. At each time, a matrix equation like Equation (A-33) will be constructed. This is the expanded form of Equation (A-3).

LEAST SQUARES SOLUTION

Next, find the solution to the matrix equation in the same manner as was described for the PPS solution above. The state vector ΔX_p represents the difference in the solutions due to the difference between the precise and the broadcast ephemerides. The improved position is the sum of the PPS solution and the deltas from the state vector.

COMPARISON TO THE TRUTH

The improved position, as well as the original PPS solution, must be compared to the true position. The "truth" will be represented by on-the-fly (OTF) kinematic solutions that are referenced to an absolute point on the main range (MBRE). This point is known absolutely to within a meter. Thus,

the truth from OTF solutions of moving antennas will be known to approximately the same accuracy. The error introduced by the OTF kinematic solution is much smaller than a meter.

REFERENCES

A-1. Hermann, Bruce R.; Evans, Alan G.; Law, Christopher S.; and Remondi, Benjamin W., "Kinematic On-The-Fly Positioning Relative To A Moving Reference," *Proceedings of the ION GPS-94*, Salt Lake City, UT, 23 Sep 1994.

A-2. Braasch, Michael S., "A Signal Model for GPS," *NAVIGATION*, Vol. 37, No. 4, Winter 1990-1991.

A-3. Hatch, Ron,"The Synergism of GPS Code and Carrier Measurements," *Proceedings of the Third International Geodetic Symposium on Satellite Doppler Positioning*, New Mexico State University, Feb 1982.

A-4. NAVSTAR GPS Space Segment/Navigation User Interfaces, ICD-GPS-200, 25 Jan 1983.

A-5. Burgess, Treva D., *OMNIS User's Guide*, Naval Surface Warfare Center, Dahlgren Division, 5 Oct 1989.

A-6. NAVSTAR GPS Space Segment/Navigation User Interfaces, ICD-GPS-200, Paragraph 20.3.3.4.3, 25 Jan 1983.

A-7. Carr, John, *The Mathematical Formulation for the Corrector/Editor Section of the OMNIS General Purpose Orbit Determination Program*, Internal K10 report, NSWCDD, date.

A-8. Goad, Clyde C., *Wallops Island Tropospheric Refraction Study and Analysis*, NASA/Wallops Station, Planetary Sciences Department No. 004-74, 12 Jul 1974.

A-9. Gibson, L. Ralph, *A Derivation of Relativistic Effects in Satellite Tracking*, NSWC TR 83-55, Apr 1983, Dahlgren, VA.

APPENDIX B

SITE 85401 DOCUMENTATION

WORLD GEODETIC SYSTEM 1984 (WGS 84)

STATION NAME	LATITUDE (deg min sec)	LONGITUDE (deg min sec)	ELLIPSOID HEIGHT(m)
85401	38 37 39.990N	90 13 19.834W	133.545

The position of station **85401** is relative to absolute station **USAF3 1988**.

Accuracy of the Positions and Ellipsoid Heights

The position of the primary control station **USAF3 1988** is estimated to have the **absolute** accuracy of ±1 meter (one-sigma) in each component (latitude, longitude, ellipsoid height), with respect to the WGS 84 datum.

The position of station **85401** is estimated to have the **relative** accuracy of ±0.02 meter (one-sigma) in each component, with respect to station **USAF3 1988**.

DISTRIBUTION

Copies

DOD ACTIVITIES (CONUS)

DEFENSE TECHNICAL INFORMATION CTR
8725 JOHN J KINGMAN ROAD
SUITE 0944
FORT BELVOIR VA 22060-6218 2

ATTN CODE E29L
(TECHNICAL LIBRARY) 1
COMMANDING OFFICER
CSSDD NSWC
6703 W HIGHWAY 98
PANAMA CITY FL 32407-7001

ATTN B ROTH 1
S MALYS 1
DEFENSE MAPPING AGENCY
4600 SANGAMORE ROAD
BETHESDA MD 20816-5003

NON-DOD ACTIVITIES (CONUS)

ATTN GIFT AND EXCHANGE DIV 4
LIBRARY OF CONGRESS
WASHINGTON DC 20540

THE CNA CORPORATION
P O BOX 16268
ALEXANDRIA VA 22302-0268 1

INTERNAL

E231		3
E282	SWANSBURG	1
K		1
K10		1
K12		1
K12	HERMANN	5
K12	SWIFT	1
K13		1
K14	RISINGER	5